AMERICAN UNIVERSITY OF BEIRUT

# SYNTHESIS, CHARACTERIZATION AND APPLICATIONS OF SURFACE-MODIFIED AND MOLECULARLY-IMPRINTED SILICA AEROGELS

by
NAIM CAMILLE SAAD

A thesis
submitted in partial fulfillment of the requirements
for the degree of Master of Science
to the Department of chemistry
of the Faculty of Arts and Sciences
at the American University of Beirut

Beirut, Lebanon
May 2014

AMERICAN UNIVERSITY OF BEIRUT

# SYNTHESIS, CHARACTERIZATION AND APPLICATIONS OF SURFACE-MODIFIED AND MOLECULARLY-IMPRINTED SILICA AEROGELS

by

NAIM CAMILLE SAAD

Approved by:

Dr. Houssam El-Rassy, Associate Professor
Chemistry — Advisor

Dr. Antoine Ghauch, Associate Professor
Chemistry — Member of Committee

Dr. Digambara Patra, Associate Professor
Chemistry — Member of Committee

Date of thesis defense: May 9th, 2014

# AMERICAN UNIVERSITY OF BEIRUT

# THESIS, DISSERTATION, PROJECT RELEASE FORM

Student Name: Saad Naim Camille
Last First Middle

(X) Master's Thesis ( ) Master's Project ( ) Doctoral Dissertation

[X] I authorize the American University of Beirut to: (a) reproduce hard or electronic copies of my thesis, dissertation, or project; (b) include such copies in the archives and digital repositories of the University; and (c) make freely available such copies to third parties for research or educational purposes.

[ ] I authorize the American University of Beirut, **three years after the date of submitting my thesis, dissertation, or project,** to: (a) reproduce hard or electronic copies of it; (b) include such copies in the archives and digital repositories of the University; and (c) make freely available such copies to third parties for research or educational purposes.

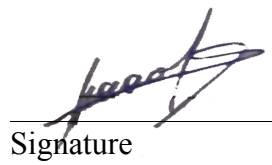

19-05-2014

Signature Date

# ACKNOWLEDGMENTS

First and foremost I would like to give thanks to my advisor Dr. Houssam El-Rassy for his incomparable patience, guidance by example, and thoughtful criticism. He taught me the value of perseverance, hard work and dedication, and thinking outside the box. I accredit the level of my degree to his support and without him this thesis would not have been fulfilled or written.

I would also like to record my gratitude to the committee members Dr. Digambara Patra and Dr. Antoine Ghauch for their constructive comments on this thesis and for their assistance, advice and helpful discussions in the experimental work.

I convey special acknowledgement to Mrs. Lara Abramian, Mr. Adnan El-Ruzz, and Mr. Boutros Ghandour for always being ready with a solution to any problem I could not solve by myself. And I would like to give a special mention to Mr. Issam Sleiman for his support and assistance with the administrative tasks necessary for completing my master program.

In my daily work I have been blessed with an ever-present group of friends who are too many to thank individually. However, a special mention goes out to Mahmoud, Mazen, Elias, Dany, Rachelle, Ali and of course Ana for the sleepless nights we were working together in the core lab, discussing matters sometimes even we didn't fully comprehend and most of all for providing a special atmosphere where the boundaries of work and play were always intermingled.

I would also like to thank all the staff at the KAS CRSL core lab, for their countless efforts in assisting me with the machines when times got rough.

Finally, and above all, I thank my parents and sisters whose love, support, and eternal confidence in me has proved to be the final push without which this work would never have been completed.

# AN ABSTRACT OF THE THESIS OF

Naim Camille Saad for Master of Science
Major: Chemistry

Title: Synthesis, characterization and applications of surface-modified and molecularly-imprinted silica aerogels

We report herein the synthesis, characterization and application of surface-functionalized and molecularly-imprinted silica gel materials. Surface-functionalized silica aerogels and alcogels prepared via a two-step sol-gel process through the combination of different silicon precursors were used in the adsorption of methylene blue from aqueous media. The effect on adsorption in batch reactors of the precursors nature, the solvent used in the adsorbents synthesis, and the pH of the dye solution was monitored. Phenyl-functionalized silica materials revealed the highest adsorption capacity. Two phenyl-modified silica aerogels were widely tested in adsorption under various experimental conditions where the effect of pH, temperature, particle size, contact time, initial dye concentration, and adsorbent dose were investigated. The synthesis solvent was found to have a clear effect on the behavior of the adsorbent whose particle size affects crucially its adsorptive capacity. pH 8 and 9 were revealed optimal and the adsorption kinetics follow a pseudo-second order representative of a co-existence of chemisorption and physisorption processes. The adsorption data fits the Sips isotherm and reveals a maximum adsorption capacity for the best aerogel $49.2 \pm 0.1$ mg of dye per gram of adsorbent. The thermodynamic study revealed the adsorption to be an exothermic and ordered adsorption process.

Molecularly-imprinted silica alcogels and aerogels with caffeine and 2-naphthol were used in the specific targeted adsorption of theophylline and PAHs from aqueous media. The effect on adsorption in batch reactors of the precursors nature, template molar ratio, water to silica ratio, light and adsorbate nature was investigated. Phenyl functionalized silica aerogels were revealed to be the best materials, imprinted with 0.075 molar ratio of template. The water to silica ratio was found to play a crucial effect on adsorption, where a ratio that provides a balance between adsorptive capacity and selectivity is closer to be found. Light was also found to have a pronounced effect on the PAH solution, engaging in a photochemical reaction with the adsorbate. The effect of the adsorbate itself was found to be of paramount importance where caffeine and 2-naphthol showed the best results. Finally, successful selectivity experiments were performed indicating that the gels present some affinity towards their target molecule.

# CONTENTS

# ILLUSTRATIONS

Figure Page

# TABLES

Table Page

# ABBREVIATIONS

| | |
|---|---|
| Acetone | Ac |
| Acetonitrile | ACN |
| Ambient pressure drying | APD |
| Aminopropyltrimethoxysilane | APTMS |
| Aminopropyltriethoxysilane | APTES |
| Caffeine | Caff |
| Dimethyl sulfoxide | DMSO |
| Dimethyl formamide | DMF |
| Double distilled water | DDW |
| Ethanol | EtOH |
| Fourier-transform infrared | FTIR |
| High performance liquid chromatography | HPLC |
| High temperature supercritical drying | HTSCD |
| Hours | h |
| Low temperature supercritical drying | LTSCD |
| Methanol | MeOH |
| Methylene blue | MB |
| Methyltriethoxysilane | MTES |
| Methyltrimethoxysilane | MTMS |
| Minutes | min |
| Molar ratio | MR |

| | |
|---|---|
| Molecularly-imprinted polymer | MIP |
| Percent adsorption | %Ads |
| Phenyltriethoxysilane | PhTES |
| Phenyltrimethoxysilane | PhTMS |
| Poly-aromatic hydrocarbon | PAH |
| Polyethoxydisiloxane | PEDS |
| Polyethylene glycol | PEG |
| Polyvinyl alcohol | PVA |
| Pore volume | PV |
| Scanning electron microscopy | SEM |
| Specific surface area | SSA |
| Standard temperature and pressure | STP |
| Tetraethoxysilane | TEOS |
| Tetrahydrofuran | THF |
| Tetramethoxysilane | TMOS |
| Theophylline | Theo |
| Trimethylsilyl chloride | TMCS |
| Ultraviolet-visible | UV-VIS |
| Vinyltriethoxysilane | VTES |
| Vinyltrimethoxysilane | VTMS |
| Water to silica ratio | R |

# CHAPTER I

# INTRODUCTION

These days, breakthroughs have become a mundane phenomenon; for many, interest in them peaks for a little and then quickly fades away. Rare are those breakthroughs that seem to be evolving and growing to benefit Mankind and the world it inhabits.

One breakthrough though, was able to withstand the test of time quite admirably: the **aerogel**! Nowadays, that word can be found really easily for anyone who is looking for it and knows what it means, whether on the sides of Dunlop tennis rackets, a NASA expedition where space dust needs to be collected, or even any daring engineering project with bold new insulation ideas. In fact, it sounds like the miracle cure to many of the challenges we are faced with on a daily basis, from tennis elbow (a common injury tennis players are more than familiar with, caused by the vibrations of the tennis racket upon impact with the tennis ball), having clean drinkable water, living in a house well insulated from both heat, cold, sound, electricity and so on.

My discussion will focus on silica aerogels, being among the most widely used materials in most fields due to their relatively inexpensive cost of preparation and ease of synthesis, all the while offering numerous benefits. Patel *et al.* said it best in comparing the aerogel to a hologram, appearing to be a projection rather than an actual solid [1], earning it the more common name of **solid smoke**. Perhaps the most fascinating aspect to this material is the fact that more than 95% of its volume is nothing

but thin air, and the remaining 5% is an interconnected matrix of silicon dioxide [1, 2]. Made through a synthesis route called the sol-gel process [3], this material offers among others an extremely high surface area, very high porosity and very low density, making it hugely appealing for a wide range of applications [1, 2].

**A. Quick Historical Sketch**

Interest in the sol-gel processing of ceramics first started in the mid 1800s with Ebelman and Graham's studies on silica gels [4]. Among the first breakthroughs was the observation that hydrolysis of tetraethoxysilane (TEOS) under acidic conditions gave a glass like material determined to be silicon dioxide ($SiO_2$) [5]. However, many disadvantages, first of which were extremely long drying times of 1 year or more [4], prevented this breakthrough from having any technological impact.

New phenomena in the period ranging from the mid 1800s to the 1920s, and mainly Liesegang rings forming from gels renewed interest in this field, and a lot of prominent figures in chemistry such as Liesegang, Ostwald and Lord Rayleigh delved deep in the study of gels and crystal growth from gels [4]. This lead to a large volume of literature on the subject but still relatively little understanding of the physico-chemical aspect of the process and final material was a setback. However, the potential of the sol-gel method was starting to gain much recognition, and the 1950s and 1960s witnessed several important milestones being crossed: Roy and coworkers (1956) used the sol-gel method to synthesize novel ceramic oxide compositions, involving new metals such as Al, Si, Ti, and Zr [6-8] that were impossible to achieve through traditional ceramic powder methods. At the same time, Iler (1955) was able, through

some never-before seen work in silica chemistry, to make colloidal silica powders commercially available [9].

Moreover, Stober et al. continued on Iler's discoveries and were able to regulate both the size and morphology of the silica powders yielding the so-called Stober spherical silica powder (figure 1.1) [10]. Ultimately, Overbeek and Sugimoto were able to produce mono-disperse colloidal silica particles [11, 12], thus breaking new ground in the field, and paving the way for scientists to keep working on it up until this very day. A colloid is a suspension in which the dispersed phase is so small (1-1000 nm) that gravitational forces are negligible and interactions are dominated by short-range forces, such as van der Waals attraction and surface charges [3]. The inertia of that dispersed phase is so small that it exhibits **Brownian motion** (or Brownian diffusion): a random walk driven by momentum from collisions with molecules of the suspending medium [2, 3].

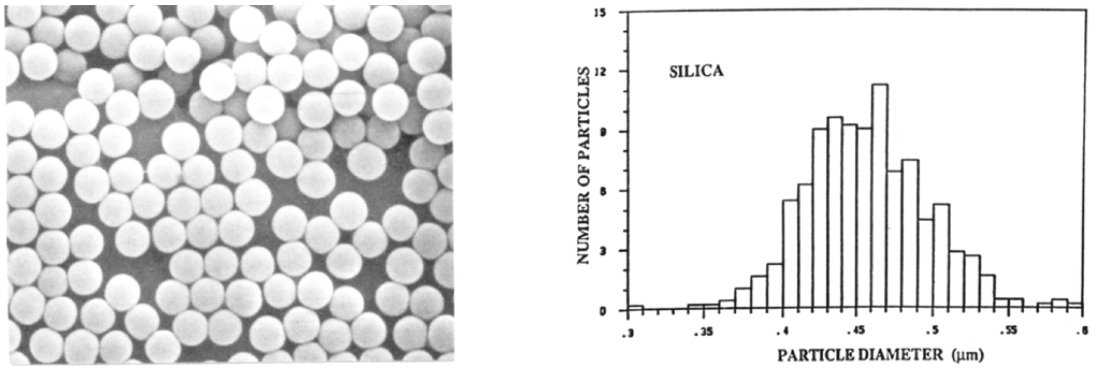


**Figure 1.1.** Left: SEM of Stober spherical silica powders. Right: Histogram (number of particles in a given diameter class versus a particle diameter) of a typical batch of Stober spherical silica powders [4].

Broadly defined, a gel is a colloid in which the solid disperse phase forms a network in combination with the fluid continuous phase, resulting in a viscous semi-rigid sol. Over time the gel starts losing in its viscosity component, and compensating

by gaining in its rigidity aspect. In the case of silica gels, usually after a period of 24 h where the gel is left to dry, what remains is a material rigid enough to stand on its own, but still containing a fairly large amount of liquid, usually an alcohol, earning it the name of **alcogel**.

However, in time, as the gel was left to stand, the liquid inside it would begin evaporating. And as it does so, the gel would start to shrink and harden, and its pores would shrink substantially as well until eventually turning into a substance that has roughly the same feel and physico-chemical properties as normal glass: the **xerogel**. All the advantages of this extremely porous high-surface-area low-density material were thus lost within a period roughly amounting to a fortnight. That is the reason why interest in gels, and mainly those resulting from the sol-gel process never really picked up as one would expect for such a novel product with such high potential.

That is until the 1930s, with Samuel Stephens Kistler: he postulated that if one would replace the liquid inside the gel with a gas with only slight shrinkage of the gel, the structure would remain intact over time [2]. Kistler thus first brought to light the concept of the **aerogel**. He was able to successfully apply his theory in synthesizing silica aerogels at first, and then driven by that success, he expanded his new technique to a wide spectrum of materials thus making aerogels out of alumina, tungsten oxide, ferric oxide, tin oxide, nickel tartrate, cellulose, cellulose nitrate, gelatin, agar, egg, albumin and even rubber [2]. As impressive as it seemed, the topic did not fire well, and the interest generated by it soon died out because of Kistler's very tedious and time consuming method to bring forth his final product: it was simply not worth it.

It wasn't until 1968, when a team of researchers in the University Claude Bernard, Lyon, France, headed by professor S. J. Teichner introduced the concept of

supercritical drying: the sol-gel process was carried out in a solvent as usual, but that solvent was then subsequently removed under supercritical conditions [2]. This method was extremely easy and fast, and Teichner et al. opened the floodgates for materials such as aerogels to be fully explored.

**B. The sol-gel process**

Sol-gel processing over the years has become an increasingly popular and reliable methodology for the synthesis of materials, especially metal oxides with uniform, small particle sizes and varied morphologies [13, 14]. In a nutshell, sol-gel processing simply involves the transition from a liquid "sol" (a colloidal suspension of solid particles in a liquid) into a solid "gel" phase, a process that can generally be divided into the following rough steps: formation of a solution, gelation, aging, drying and finally densification [2]. The advantages such a method has to offer are plenty: extremely simple synthesis, economic, effective, and produces high quality materials are just to name a few.

Before going any further, it is essential to properly define the word **gel** in the context in which it will be used in this work: an interconnected, rigid network with pores of sub micrometer dimensions and polymeric chains whose average length is greater than a micrometer [4]. **Gelation** can be defined as the process by which a free-flowing sol is converted into a 3D solid network enclosing the solvent medium. In simple terms, a gel is nothing else than a semisolid rich in liquid [2]: the liquid does not allow the solid network to collapse while the latter does not allow the liquid to flow out [15]. The exact moment at which gelation occurs is most generally identified by an

abrupt change in viscosity and an elastic response to stress, a point most conveniently induced by a change in the pH of the reaction solution [2].

Many approaches have been proposed over the years to make sol-gel monoliths, of which the hydrolysis and polycondensation of alkoxide precursors followed by aging and drying under ambient atmosphere [4] is proving to be the one having the most success, and will be the method used in this work. The generation of inorganic sols requires controlled conditions, making them stable with respect to agglomeration and precipitation. To that end, several factors can be controlled, monitored and regulated to manipulate and fine-tune the formation of the sol, such as polarity of the solvent, ionic strength of the reaction medium and temperature just to name a few.

**C. The chemistry behind the sol-gel process: Synthesis**

The synthesis of silica gels can be divided into three general steps [16]. First: the **gel preparation** step in which silicon alkoxides are mixed with a solvent and a catalyst. Through an induced changed in pH, gelation is obtained. The dispersion medium used in the synthesis usually classifies the resulting gels: hydrogel or aquagel, alcogel and aerogel (for water, alcohol and air respectively). The second step is the all-important **aging** of the gel, in which the material is aged in its mother solution, thus strengthening the gel so that shrinkage during the third and final drying step is kept to a minimum. Finally, the **drying** of the gel is the crucial final step to this synthesis procedure, in which the gel is freed of its pore liquid. To prevent the shrinkage and ultimately collapse of the gel structure during drying, special conditions need to be met and rigorously observed.

### *1. Gel preparation*

a. Starting materials: *The Precursors*

Precursors must satisfy two important requirements: they must be soluble in the reaction media and should be reactive enough to participate in the gel forming process [17]. Metal alkoxides (in our case silicon alkoxides) are **metal-organic** compounds, which have an organic ligand attached to a metal or metalloid atom [3]. They are popular precursors because they react readily with water in a hydrolysis reaction, where a hydroxyl ion becomes attached to the metal atom according to the following reaction:

$$Si(OR)_4 + H_2O \rightleftharpoons HO - Si(OR)_3 + ROH \qquad (1.1)$$

The most common alkoxysilane precursors are tetramethoxysilane (TMOS) and tetraethoxysilane (TEOS).

TMOS, as well as many other silicon alkoxides, have been studied thoroughly and extensively over the years to produce monolithic silica aerogels [18-23]. However, silicon alkoxides are extremely hazardous and toxic materials, with deleterious health effects. They are also very expensive [16]. Those two reasons steer the scientific community into trying to find safer and more commercially accessible alternatives for silicon aerogel precursors, but silicon alkoxides remain nonetheless (at least for the present and near future) the main precursors for silica aerogel synthesis.

b. Sol preparation and gelation

Over the years, different scientists and investigators have used several procedures for different preparations of different silica aerogels [24-36]. However, the

synthesis of silicate materials followed a well-defined general route that begins by the hydrolysis of monomeric tetra-functional and tri-functional silicon alkoxide precursors, employing either an acid or a base as a catalyst. Next comes the polycondensation step in which the silicon precursors begin to form networks and crosslinks which will later become the backbone of the gel itself once the third step (aging of the gel) is done. The following schemes depict the sol-gel reactions that occur during silica network formation [2, 37]; hydrolysis in equation (1.2), and water and alcohol condensation in equations (1.3) and (1.4) respectively.

$$Si(OR)_4 + 4H_2O \underset{Esterification}{\overset{Hydrolysis}{\rightleftharpoons}} Si(OH)_4 + 4ROH \tag{1.2}$$

$$\equiv Si(OH) + (OH)Si \equiv \underset{Hydrolysis}{\rightleftharpoons} \equiv Si - O - Si \equiv + H_2O \tag{1.3}$$

$$\equiv Si(OH) + (OCH_3)Si \equiv \underset{Alcoholysis}{\rightleftharpoons} \equiv Si - O - Si \equiv + CH_3OH \tag{1.4}$$

In other terms, if one wished to observe the exact reaction mechanism, it could easily be drawn as such:

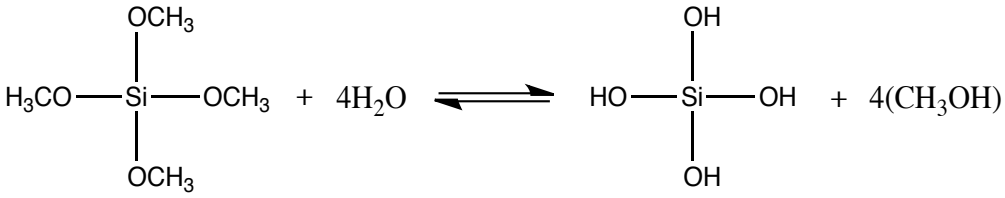


(1.5)

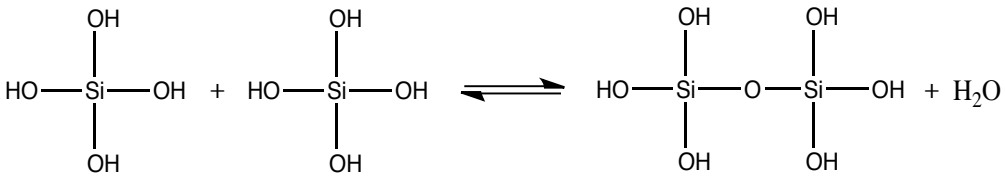


(1.6)

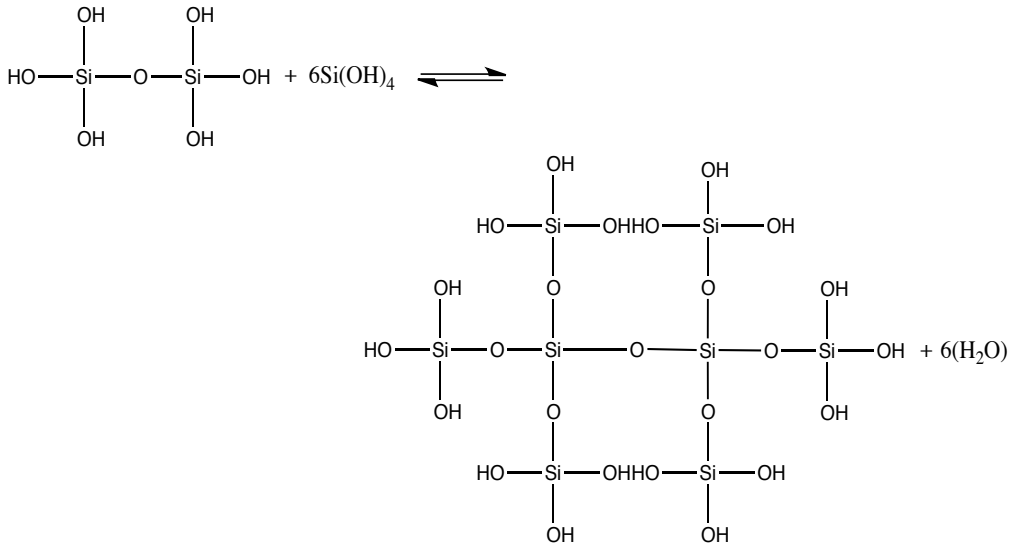


(1.7)

Equation (1.5) shows a hydrolysis reaction, equation (1.6) shows a condensation reaction, which when applied successively results into a polycondensation reaction as depicted in equation (1.7), ultimately resulting in a $SiO_2$ network. The water and alcohol expelled from the reaction remain within the pores of the network [4].

i. Hydrolysis and Condensation

The first step of the synthesis process is the mixing of the alkoxysilane precursor and water. However, these two are partially immiscible, and therefore additional solvent such as alcohol, acetone, dioxane, tetrahydrofuran (THF) and acetonitrile is needed to homogenize the mixture [16]. A phase diagram of the system alkoxysilane-water-solvent proposed by Brinker and Scherer is shown in figure 1.2 [3].

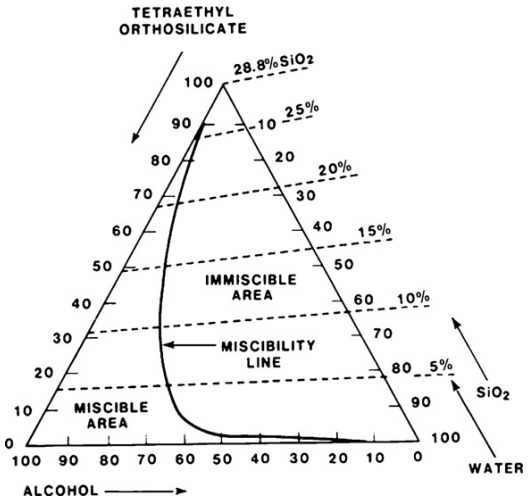


**Figure 1.2.** Ternary phase diagram of the system TEOS-ethanol-water at 25°C [3].

Hydrolysis of silicon alkoxides is a versatile technique in which varying different parameters such as the water to silica ratio [16, 34], the catalysis technique employed [16, 29, 30, 38, 39], the nature of the catalyst [40] and which types of acids and bases are used [16, 28, 35, 41-44] can produce materials with completely different physico-chemical properties.

Figure 1.3 depicts how pH affects the relative rate of reaction ($v_{rel}$) for both hydrolysis and condensation, indicating that condensation kinetics are much faster under base catalysis then hydrolysis kinetics, and vice versa.

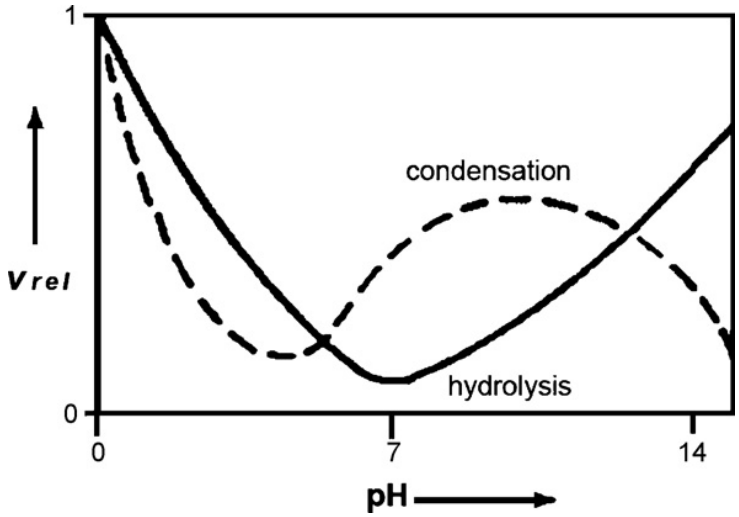


**Figure 1.3.** Dependence of the relative hydrolysis and condensation rates on the pH of the solution [16].

In general, any factor affecting the rate of hydrolysis and condensation will have an effect on the final structure of the finished material [3, 4, 45-53], since it is during these two processes that the actual structure takes shape [4].

In some cases, reports are appearing in which scientists are using additives such as polyethylene glycol (PEG) and polyvinyl alcohol (PVA) as porogens to increase the pore size and mechanical properties of the gels [36, 54, 55], a practice that is gaining in popularity.

### *2. Aging*

Aging of the gel, as process also known by the name of **syneresis**, requires keeping the cast gel for a variable amount of time (from hours to days), completely immersed in its own liquid [4]. During that time, polycondensation continues and localized dissolution and re-precipitation of the gel network is observed, driven by differences in solubility for surfaces with different curvatures, thus increasing the thickness of the inter-particle necks and decreasing the porosity of the network [4].

However, this step is of crucial importance because it increases the strength of the gel, thus allowing it to withstand drying without cracking [16, 56]. Two different mechanisms are generally accepted when it comes to the aging of a gel, operating simultaneously albeit at different rates (figure 1.4) [16]:

1. Neck growth from re-precipitation of silica dissolved from particle surface onto necks between particles.
2. Dissolution of smaller particles and precipitation onto larger ones.

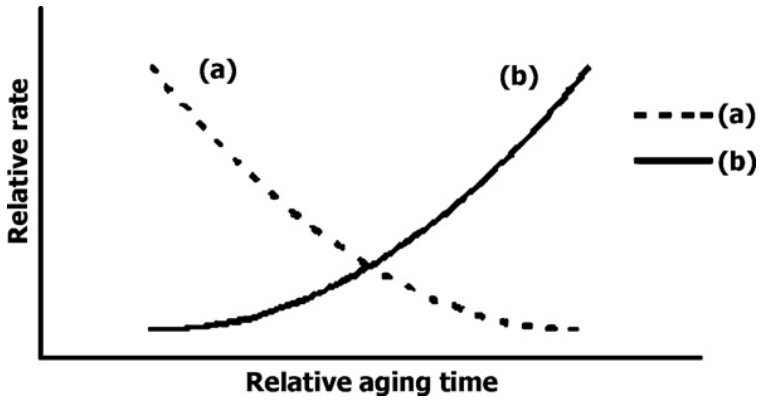


**Figure 1.4.** Relative aging rate as a function of time for two aging mechanisms: (a) Re-precipitation of silica dissolved from the particle surfaces onto the necks between particles. (b) Re-precipitation of small dissolved silica particles onto larger ones [57].

### *3. Drying*

The drying step is the most crucial step in the synthesis of aerogels. It is the only aspect distinguishing aerogels from all other similar materials. This seemingly simple move is actually the hardest and most critical one because of **capillary forces** that set up in the fine pores by the liquid vapor interface [2]: the smaller the capillary radius, the higher the liquid will rise, and thus the higher the hydrostatic pressure. This drives the gel to shrink during drying. The capillary pressure can be represented by:

$$P_c = \frac{-\gamma_{lv}}{(r_p - \delta)} \tag{1.8}$$

where $\gamma_{lv}$ is the surface tension of the pore liquid, $r_p$ is the pore radius (represented in equation 1.9 below) and $\delta$ is the thickness of a surface absorbed layer [3, 58].

$$r_p = \frac{2V_p}{S_p} \tag{1.9}$$

where $V_p$ and $S_p$ are pore volume and surface area, respectively. They are critical parameters, as it is the gradient in the capillary pressure within the pores that leads to mechanical damage; the capillary pressure developed during the drying (reaching up to 100-200 MPa) causes shrinkage and cracking. Also, very small pore sizes induce fracture during drying due to those enormous forces [59].

a. Supercritical drying (SCD)

Two main categories of supercritical drying exist: high temperature supercritical drying (HTSCD) first developed by Kistler in 1931 and low temperature supercritical drying (LTSCD) who saw the light with Teichner in 1968. In HTSCD the wet gel is placed in an autoclave along with a sufficient amount of solvent and the temperature is slowly raised, causing as well a raise in the pressure. Both temperature and pressure are constantly monitored and adjusted to reach values above the critical points of the solvent in use. Once reached, the temperature and pressure are kept constant for a period of time then the fluid is slowly vented at constant temperature, causing the pressure to drop. Finally, when ambient pressure is reached, the temperature is brought down to room temperature. In that way, the phase boundary between liquid and gas is not crossed at any point of the drying process (figure 1.5a). However, the

high pressures and temperatures reached represent, apart from the physical danger, many challenges as well as they alter the chemical composition of the gel. A lot of research has gone into HTSCD to reduce those risks [16, 60-63], but none so far have been able to accomplish it.

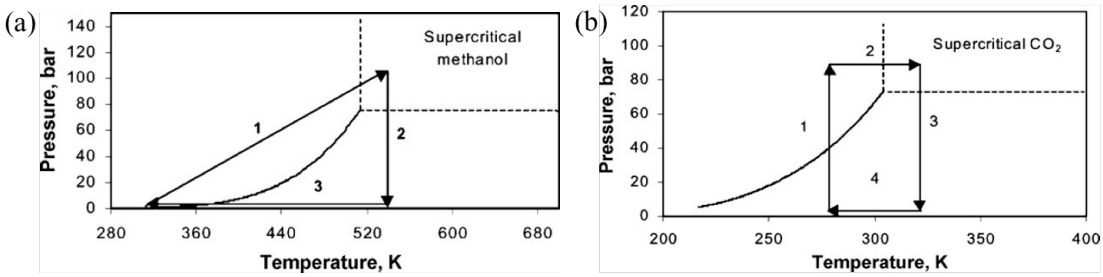


**Figure 1.5.** Schematic procedure of (a) high temperature and (b) low temperature supercritical drying processes [16].

LTSCD is very similar to HTSCD in theory, with the addition of one crucial step: solvent exchange. Chemists replaced (exchanged) the alcohol (or any other solvent) in the gel by a liquid with a critical point close to ambient temperature. To that end, liquid $CO_2$ was found to be the most practical choice [16]. The main advantage of that method is that it is implemented at low temperatures (generally less than 40°C) and moderate pressures (less than 80 bar), thus lowering the risk both to man and gel, even if it means adding an extra step to the synthesis procedure (figure 1.5b). Of course, and as with the HTSCD, the process has been studied extensively and modified to tailor to specific ends [16, 64].

Aerogels resulting from HTSCD and LTSCD have slightly different characteristics, such as pore volume [65, 66] and surface chemistry [28, 65], but comparable optical activity [65, 67, 68].

b. Ambient pressure drying (APD)

APD involves the evaporation of the solvent contained within the gel at ambient pressures. To that end, special measures need to be put in place so that the solvent could be evaporated out without damaging the gel structure. To achieve this, the surface of the gel needs to be modified, the network needs to be strengthened and the contact angle between the pore liquid and the pore walls has to be influenced [16]. To that end, silylation was found to be an effective method to chemically modify the inner surface. After solvent exchange with one of higher vapor pressure, drying happens by simple evaporation of the solvent.

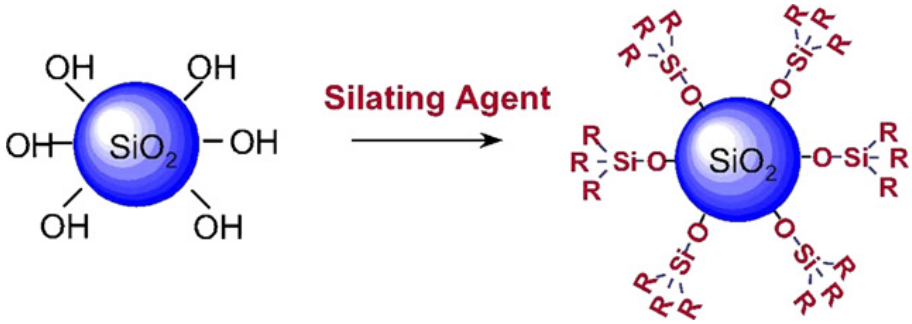


**Figure 1.6.** Silylating of silica gel [16].

While a chemically and economically more attractive alternative to supercritical drying, this process requires long periods of time and large amounts of

solvents for the exchange, as well as the omnipresent risk of cracking. However, when done properly, it can result in gels having densities as low as 0.150 g/cm$^3$, and total pore volumes even larger than those obtained for corresponding gels dried via the low temperature $CO_2$ supercritical drying method [69].

c. Freeze-dying

In this method, the phase boundary between liquid and gas is removed altogether, meaning that capillary pressure does not play a fundamental role [16]. The solvent is exchanged for one with low expansion coefficient and high sublimation pressure, then the pore liquid is frozen and sublimed under vacuum to obtain a material referred to a **cryogel** [16]. This is the least appealing of all drying methods, as the disadvantages largely outweigh the benefits. These include but are not limited to a prolonged aging period necessary for the stabilization of the network and destruction of the network altogether by crystallization of the solvent molecules inside the pores [16].

**D. Properties and broad applications of silica aerogels**

The properties of aerogels make them extremely attractive materials and are the reason behind their enormous success in the many fields they are applied in. These properties are regrouped in table 1.1. Figure 1.7 provides as well some insight deep inside the pores of typical silica aerogels, showing their pore characteristics through scanning electron microscopy (SEM) and transmission electron microscopy (TEM).

**Table 1.1.** Typical properties of silica aerogels taken from Dorcheh and Abbasi [16].

| Property | Value | Comments |
|---|---|---|
| Apparent density | 0.003 - 0.35 g/cm$^3$ | Most common density is ≈ 0.1 g/cm$^3$ |
| Internal surface area | 500 - 1000 m$^2$/g | |
| %Solids | 0.13 - 15 % | Typically 5% (95% free space) |
| Mean pore diameter | ≈ 20 nm | As determined by BET method |
| Primary particle diameter | 2 - 5 nm | Determined by electron microscopy |
| Refreactive index | 1.0 - 1.08 | |
| Coefficient of thermal expansion | 2.0 - 4.0 × 10-6 | Determined using ultrasonic methods |
| Dielectric constant | ≈ 1.1 | For a density of 0.1 g/cm$^3$ |
| Sound velocity | 100 m/s | For a density of 0.07 g/cm$^3$ |

And as is well seen in figure 1.7 below, the surface structure of the materials is uniform both in size and distribution. These impressive properties give rise to numerous applications (figure 1.10).

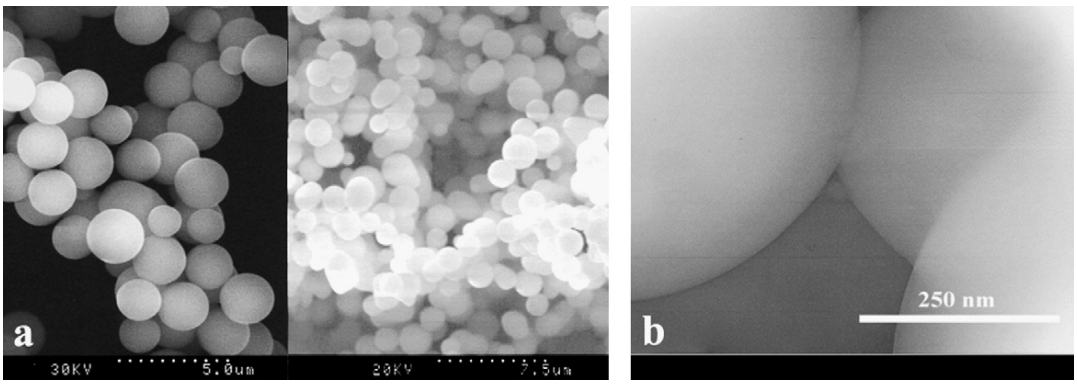


**Figure 1.7.** (a) SEM; (b) TEM picture, showing the pore characteristics of silica aerogels [16].

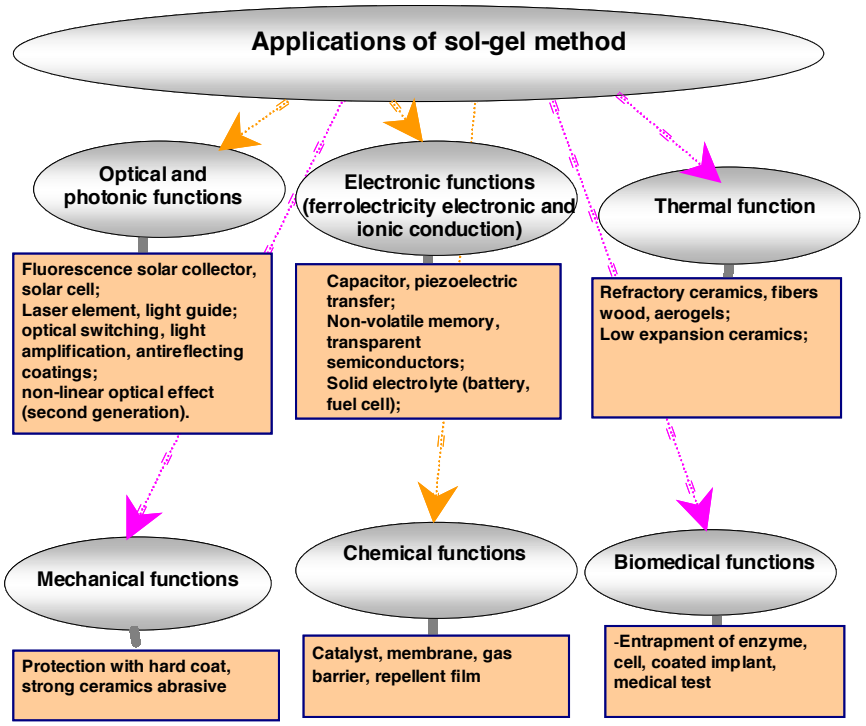


**Figure 1.8.** Selection of some main applications of silica aerogels [70].

## E. Surface-functionalized sol-gel materials

Surface functionalized silica materials obtained through the sol-gel process can be viewed as silica-based organic-inorganic hybrids. They are attractive composite materials due to the fact that they combine in a single solid both the properties of a rigid three-dimensional silica network with the particular chemical reactivity of the organic components [71-74]. These multifunctional materials have found numerous applications in various fields, most relevant of which are chemical and biological sensors, separation sciences, optical devices, catalysis [75-77] , and electrochemistry [78]. Surface functionalized silica gels can be classified into two categories [78]: class I materials, characterized by weak interactions between the organic and inorganic components (hydrogen bonding, van der Waals contacts, or electrostatic forces), and class II

materials where the organic and inorganic components are linked through strong chemical bonds (covalent, ionic, or Lewis acid–base bonds). The latter is the one of most interest in most fields due to its higher stability and stronger structure [78].

These materials can be prepared either by post-synthesis grafting of the surface of unmodified silica with organofunctional alkoxysilanes or chlorosilanes, or in one step by co-condensation of silicon alkoxides and one or more organosilanes [78]. The ease of synthesis and versatility of the finished solid materials thus providing a wide range of organically-modified silica-based materials resulted in a big boost in the field during the last decade [78, 79]. Another important breakthrough in materials science relies on the use of supramolecular templating techniques, thus building mesoporous silica architectures around self-assembled organic templates. These ordered solids can also be designed in the form of organic–inorganic nanocomposites, once functionalized with suitable organosilane reagents [80, 81].

The versatility of the sol–gel process allows the production of composite materials in various morphologies (i.e. xerogels, alcogels, aerogels, thin and thick films, uniform particles, monoliths) displaying tailor-made chemical, mechanical, optical, or electrical properties [78]. Moreover, the ‘‘soft’’ conditions associated with the sol–gel process have been proven to be compatible with the immobilization of biomolecules (i.e., enzymes) by encapsulation in silica-based materials without preventing their biological activity, leading to various applications in the field of biosensors [82-84].

Surface-functionalized silica gels are extremely attractive materials for many applications. They are usually highly porous solids made of a mechanically stable inorganic backbone having large specific surface areas likely to contain a high number of organic functional groups accessible to external reagents or analytes. Open

frameworks enable effective and fast access to these functional groups. One such application could be the removal of dyes in wastewater by adsorption onto silica sol-gel materials.

### *1. Surface-functionalized sol-gel materials as dye adsorbents from wastewater*

Synthetic dyes are extensively used in many areas of today's technologies, from textile [85] to leather [86], paper production [87], food technology [88], agricultural research [89], light harvesting arrays [90], photoelectrochemical cells [91] all the way to hair colorings [92]. While these synthetic dyes possess a wide range of structural diversity, the bulk that is being used in the industry belongs to the category of azo-aromatic dyes [93]. In recent years, the huge discharge of organic dyes in the hydrosphere from the various anthropogenic sources listed above (estimated to be over 10,000 tons per year [93]) is starting to represent an increasing danger for the environment and human beings alike as they contribute, besides the aesthetic pollution, to significant water toxicity. Figure 1.10 shows one such incident happening in the Beirut river in 2012.

**Figure 1.9.** Pictures showing Beirut river turning blood red due to a red colorant being dumped into it. *(Pictures taken from the daily star on February 15th, 2012: http://www.dailystar.com.lb/)*

Indeed, synthetic dyes are known to be among others toxic, carcinogenic, mutagenic [94], and concentrations as low as 1 ppm are clearly visible to the human eye [95]. Therefore, the removal of these dyes is rapidly becoming a big priority from an environmental and health point of view. However, these molecules possess large sizes and high stability as non-biologically degradable entities. Numerous techniques such as physical, biological and chemical conventional techniques (many of which proved to be a complete failure [96]) were previously used to remove these pollutants from aqueous media, such as adsorption, photocatalytic degradation, chemical decomposition by oxidation, and microbiological discoloration [93, 97]. Out of these processes, the physical adsorption at the solid-liquid interface has always stood out as an efficient and economically appealing practice for decreasing the concentration of dyes in effluent wastewater due to its easiness, low cost, and the availability of a wide array of adsorbents to choose from. Among these, metal oxide sol-gel materials [3] appear to be adsorbents with very high potential due to the ease in which their porosity and surface properties can be controlled. This helps in adjusting their affinity to specific adsorbates. Recent studies focused on the use of alumina [98], silica [96, 99-101], and titania [94] sol-gel materials as adsorbents for pollutants from wastewater.

In this study (third chapter of this manuscript), we investigate the effect of phenyl and vinyl surface modification of silica aerogels and alcogels on the removal of methylene blue dye from aqueous media. This molecule was selected for this study because it is widely and commonly used in the textile industry, as well as having applications in medicine and spectroscopy [99]. This heterocyclic aromatic dye molecule can cause many well-documented threats to both human beings and animals such as severe and sometimes permanent eye injury, difficult breathing when inhaled,

undesirable and harmful symptoms ranging from burning sensations to vomiting when ingested, and mental confusion and methemoglobinemia [95, 102, 103]. Several previous studies were conducted to remove the methylene blue dye from aqueous media using various low-cost solid adsorbents. Table 1.2 regroups some of these results [102-112].

**Table 1.2.** Comparison of the maximum monolayer adsorption capacities of methylene blue onto various low-cost adsorbents.

| Adsorbent | Maximum monolayer adsorption capacities (mg/g) | Reference |
|---|---|---|
| Bamboo based activated carbon | 454.2 (30°C) | [103] |
| Swede rape straw (SRS) | 246.4 (modified with tartaric acid), 128.2 (T N/A) | [104] |
| Biosolid | ≈ 240 (25°C) | [105] |
| Green pea peel | 163.94 (30°C) | [106] |
| Carbon nanotubes | 35.4 (0°C); 46.8 (25°C); 64.7 (60°C) | [107] |
| Coconut shell activated carbon | 45.9 (28°C, KOH-treated); 41.8 (28°C, untreated) | [108] |
| Rice husk | 40.5883 (32°C) | [109] |
| Kaolinite clay | 13.99 (27°C, pure); 20.49 (27°C, NaOH-treated) | [102] |
| Coir pith carbon | 5.87 (40°C) | [110] |
| Chicken egg-shell membrane | 4.83 (80°C) | [111] |
| Oyster shell | 1.09 (25°C) | [112] |

**F. Molecular-imprinting in sol-gel materials.**

Molecular recognition is one of the basic processes in nature, and the most relevant example is right inside the human body, with the enzyme and substrate's lock and key mechanism. It can thought of as the preferential binding of a molecule to a receptor whose selectivity is much higher than that of its analogues [113]. The dream of many chemists is to bring that natural phenomenon and use it in synthetically derived materials. Since the 1930s, the innumerable applications such a material would provide

has caught the eye of scientists, and they have been trying to replicate it ever since [114-118].

Polyakov first reported that the silica pore structure was influenced by the presence of benzene, toluene or xylene during the drying process [113]. The extent of silica gel adsorption of the different solvent vapors was dependent upon the structure of the solvent present during the drying process. Selectivity was suggested to arise from changes in the silica structure induced by the presence of the particular solvent. Since then, different oxides have been imprinted in an attempt to prepare specific adsorbents, catalysts and separation media. In 1942 Pauling and Campbell [116] reported the preparation of artificial antibodies using antigen molecules as templates. In 1949, Dickey reports what appears to be the first documented demonstration of nanostructured silica gels prepared by imprinting the formation of an acidified silica solution with homologues of methyl orange [113] which, after dye extraction, adsorbed methyl orange better than a blank gel. Much later, investigations of imprinted silicas renewed, and after the 1970s imprinted sol-gel materials have been produced and applied as adsorbents, separation media, catalysts and, more recently, as sensing phases[117, 119].

Over the past few decades, research breakthroughs made in designing pharmaceutical drugs have greatly advanced the knowledge of physicochemical properties of drug molecules as well as mechanisms of cellular uptake. These breakthroughs have lead scientists to believe that the conventional treatment methods have adverse side effects and limited effectiveness due to lack of target specificity of the drug [120]. A widely pursuit solution to this problem is the design of a target-specific drug delivery system (DDS) that can transport an effective dosage of drug molecules to targeted cells and tissues [120]. Among several strategies to achieve this,

molecularly-imprinted polymers (MIPs) are one of the most widely studied materials for controlled drug uptake and release. These solids belong to a class of materials called stimuli responsive materials (SRMs), able to respond to specific external stimuli (e.g. changes in temperature, pH, ionic and/or solvent composition, concentration of specific chemical species, electric field, photo-irradiation, etc.), with a considerable change in their properties [121].

Chemically speaking, molecular imprinting is a means of introducing sites of specific molecular arrangement into an otherwise uniform polymeric matrix [121]. This is achieved through the formation of a pre-polymerization complex between complementary monomers and the template molecule, after which polymerization results in the production of a macro-porous polymer capable of specific molecular recognition [122]. Applying it in sol-gel chemistry, it is possible to synthesize a gel through the normal sol-gel process with the slight alteration of introducing a molecule serving as a **template**. That template would subsequently be removed to leave behind a cavity with complementary morphological and chemical features, thus making it highly selective towards molecules with similar stereochemistry [113]. This process is better illustrated in figure 1.10, and several imprinting routes are presented in figure 1.11, that serve as a reminder of the versatility of the sol-gel synthesis technique.

Conventional template removal techniques include calcination [123], extensive washing with alcohol/acid combinations [124, 125], or high temperature soxhlet extraction using mostly a combination of methanol/acetic acid as extraction solvent [126, 127]. However, these methods are expensive, time consuming, and occur at very high temperatures, which can lead to irreversible considerable damage for the gels, not to mention that some methods like calcination for example, do not allow aerogel

synthesis. We proposed a solution to this problem with a slight modification to the supercritical drying method, which will be discussed in subsequent sections of this work.

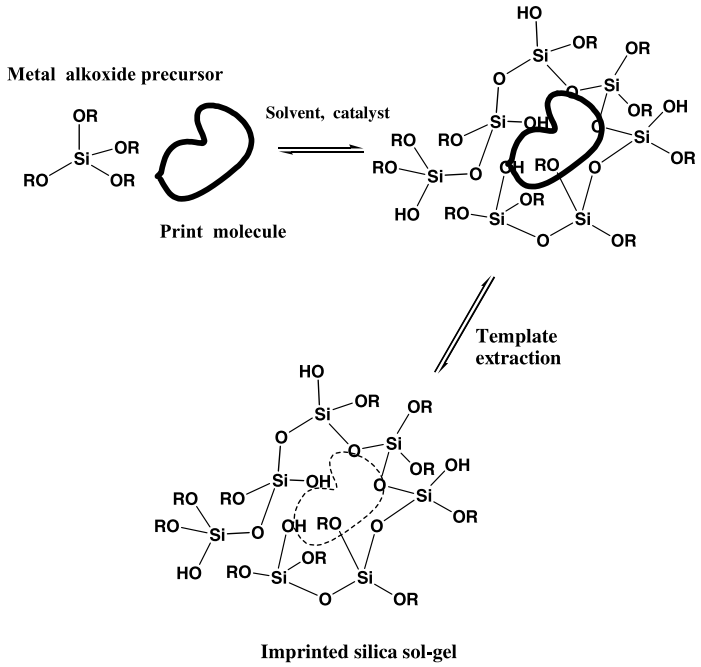


**Figure 1.10.** Non-covalent silica molecular imprinting process sequence [113].

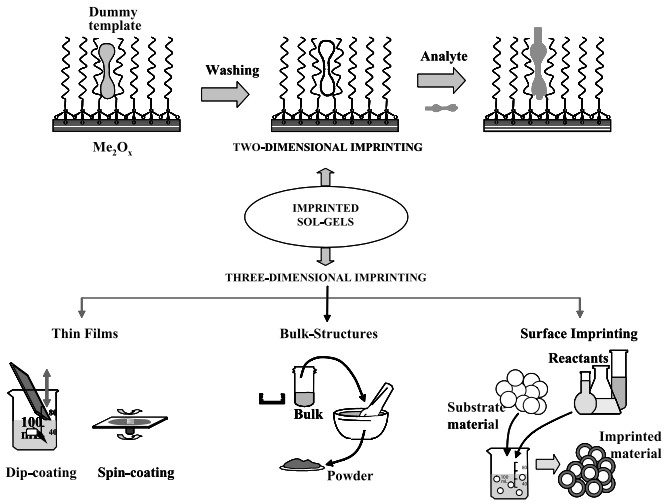


**Figure 1.11.** Different routes for sol-gel molecular imprinting [113].

Although molecular imprinting is an effective solution for drug delivery and controlled release, it is not without its drawbacks. Indeed, MIPs are still organic molecules containing solvents and functional groups that are potentially harmful to the human body. Although organic imprinted polymers have been around for a while, and recent studies have focused on the preparation of inorganic molecularly-imprinted hydrogels, to our knowledge, synthesis of inorganic molecularly-imprinted aerogels has not yet been achieved and studied. We report for the first time the synthesis of molecularly-imprinted silica aerogels, major contenders for drug delivery and controlled release applications, since they are easily manageable solids that contain no harmful solvents or functional groups.

**G. Purpose of the work**

In this work, two main projects have been explored: First the use of surface-modified silica alcogels and aerogels as sorbents for methylene blue has been investigated in an attempt to find an efficient and economically attractive solution for the removal of dyes from wastewaters. The effects of the precursors nature, the solvent used in the adsorbents synthesis, and the pH of the dye solution were monitored. The effect of temperature, particle size, contact time, initial dye concentration, and adsorbent dose were investigated. A complete kinetic and thermodynamic study was performed at optimal conditions as a first step to apply this material in industry, in filtering systems for companies using dyes in their manufacturing processes.

Second, the use of molecularly-imprinted silica alcogels and aerogels as specific adsorbents for caffeine and theophylline and polycylic-aromatic hydrocarbons

(PAHs) was investigated. The effect of precursors nature, water to silica ratio, and template to silica molar ratio were studied. Also, the effect of light on the PAH solution was analyzed. Finally, adsorption competition experiments were performed to test for selectivity. These experiments were performed as a stepping stone for medicinal applications such drug targeting and controlled release.

# CHAPTER II

# SYNTHESIS AND CHARACTERIZATION OF SILICA SOL-GEL MATERIALS FOR ADSORPTION

Surface-functionalized and molecularly-imprinted silica sol-gel materials were synthesized and tested in adsorption, to explore the effect of variation of specific parameters on their adsorptive capacity. The synthesis procedure will be explained in details in the subsequent section, followed by characterization through FTIR and SEM. Alcogels and aerogels were then tested in adsorption of methylene blue (chapter III) and specific adsorption of theophylline and PAHs (chapter IV).

## A. Synthesis of silica sol-gel materials for adsorption

### *1. Materials*

All chemicals were used in this study as received and with no further purification. Tetramethylorthosilicate ($C_4H_{12}O_4Si$, TMOS), tetraethylorthosilicate ($C_8H_{20}O_4Si$, TEOS), vinyltriethoxysilane ($C_8H_{18}O_3Si$, VTES), vinyltrimethoxysilane ($C_5H_{12}O_3Si$, VTMS), caffeine ($C_8H_{10}N_4O_2$) and anthracene ($C_{14}H_{10}$) were purchased from Fluka Analytical. Phenyltrimethoxysilane ($C_9H_{14}O_3Si$, PhTMS), phenyltriethoxysilane ($C_{12}H_{20}O_3Si$, PhTES), aminopropyltriethoxysilane ($C_9H_{23}NO_3Si$, APTES), naphthalene ($C_{10}H_8$), 2-napthol ($C_{10}H_8O$), pyrene ($C_{16}H_{10}$) and methylene blue ($C_{16}H_{18}ClN_3S$,) were purchased form Acros Organics. Theophylline ($C_7H_8N_4O_2$),

theobromine ($C_7H_8N_4O_2$) Dimethyl sulfoxide ($C_2H_6SO$, DMSO, 99.5%) and dimethylformamide ($C_3H_7SO$, DMF) were acquired from Sigma. Hydrochloric acid (HCl, 37%), sulfuric acid ($H_2SO_4$, 97%) and ammonium hydroxide ($NH_4OH$, 28.0%-30%) were from Panreac, BDH and Fischer-Scientific respectively. Methanol ($CH_3OH$, 99.9%), ethanol ($C_2H_5OH$, 99.8%), chloroform ($CHCl_3$, 99.9%) and tetrahydrofuran ($C_4H_8O$, THF) were purchased from Sigma-Aldrich, Acetone ($CH_3COCH_3$, 99%) from SureChem Products LTD, and Acetonitrile ($CH_3CN$, 99.9%) from Lab-Scan. Finally, double distilled water was prepared in our laboratory.

***2. Synthesis of alcogels and aerogels for methylene blue adsorption***

Tetraalkoxysilanes ($Si(OR)_4$; R = $CH_3$ or $C_2H_5$) were used alone in the preparation of the silica gels or combined with other silicon precursors ($R''Si(OR')_3$; R' = $CH_3$ or $C_2H_5$; R'' = $C_6H_5$ or $C_2H_3$). As well as the silicon precursors change, the synthesis solvent was also varied where methanol, ethanol, acetone, acetonitrile, DMSO, and DMF were used. Out of these 6 solvents, only 3 resulted in successful gelation of the sol: methanol, acetone and acetonitrile. The molar ratio $Si(OR)_4$:$R''Si(OR')_3$ was maintained constant at 1:0.25 whenever $R''Si(OR')_3$ precursors were used.

In the first step, silicon precursors were mixed in a polypropylene vial with the solvent, double distilled water and hydrochloric acid solution (0.2 M) under magnetic stirring for 24 h. An ammonium hydroxide solution (0.5 M) was then added and mixed together for 5 min. The vials were closed and kept for gelation and aging. The former was observed in the next 2 hours and the obtained gels were kept for aging for one day at room temperature. After this period, the wet alcogels were either used directly in the

adsorption experiments or dried under supercritical carbon dioxide ($T_c$ = 31.1 °C; $P_c$ = 73.7 bar) to obtain the silica aerogels. The supercritical drying step was preceded by a 24 h-solvent exchange step, where the alcogels were soaked in acetone in order to exchange the residual water and solvent in the gel with acetone exhibiting a higher miscibility with liquid carbon dioxide.

The final molar ratios $Si(OR)_4$:Solvent:$H_2O$:HCl:$NH_3$ were $1:12:6:3\times10^{-3}:6\times10^{-3}$ for the gels where TMOS or TEOS were used alone as silicon precursors, whereas the ratios $Si(OR)_4$:R''$Si(OR')_3$:Solvent:$H_2O$:HCl:$NH_3$ were $0.8:0.2:12:6:3\times10^{-3}:6\times10^{-3}$ for the other gels. The amount of silica was chosen to be 3 mmol, thus giving final gel volumes of 2.5 to 3 mL. Figure 2.1 gives a full synthesis scheme taking as an example gels synthesized with methanol solvent, and thus showing the difference between the surface-functionalized and non-functionalized gels.

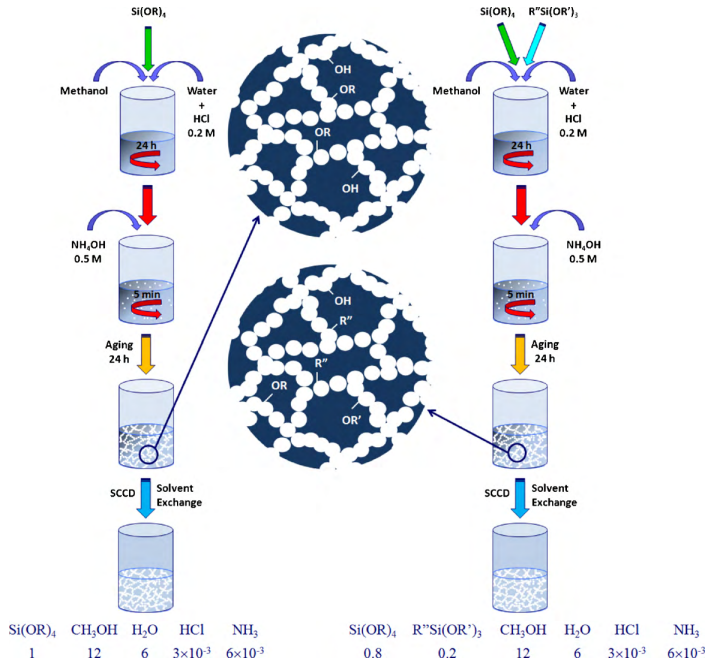


**Figure 2.1.** Flow chart illustrating the preparation of both surface-functionalized and non-functionalized silica aerogels with methanol as a solvent [128]

Following this procedure, and varying the alkoxide precursors and solvent, 18 different gels were thus synthesized, and regrouped in table 2.1 below.

**Table 2.1.** Precursor/co-precursor/solvent composition of the different surface-modified silica gels.

| Sample | Composition | Solvent | Sample | Composition | Solvent |
|---|---|---|---|---|---|
| M1 | TMOS | Methanol | E1 | TEOS | Methanol |
| M1' | TMOS | Acetone | E1' | TEOS | Acetone |
| M1" | TMOS | Acetonitrile | E1" | TEOS | Acetonitrile |
| M2 | TMOS-PhTMS | Methanol | E2 | TEOS-PhTMS | Methanol |
| M2' | TMOS-PhTMS | Acetone | E2' | TEOS-PhTMS | Acetone |
| M2" | TMOS-PhTMS | Acetonitrile | E2" | TEOS-PhTMS | Acetonitrile |
| M3 | TMOS-PhTES | Methanol | E3 | TEOS-PhTES | Methanol |
| M3' | TMOS-PhTES | Acetone | E3' | TEOS-PhTES | Acetone |
| M3" | TMOS-PhTES | Acetonitrile | E3" | TEOS-PhTES | Acetonitrile |

### *3. Synthesis of silica alcogels and aerogels for specific adsorption of theophylline and PAHs.*

Tetraalkoxysilanes ($Si(OR)_4$; with R = $CH_3$ or $C_2H_5$) were used alone in the preparation of the silica gels or combined with other silicon precursors ($R''Si(OR')_3$; with R' = $CH_3$ or $C_2H_5$; R'' = $C_6H_5$ or $C_2H_3$). The molar ratio $Si(OR)_4$:$R''Si(OR')_3$ was maintained constant at 1:0.25 whenever $R''Si(OR')_3$ precursors were used.

In the first step, silicon precursors were mixed in a polypropylene vial with the solvent, double distilled water and hydrochloric acid solution (0.2 M) under magnetic stirring for 24 h. The template material (caffeine/2-naphthol) was accurately weighed and mixed also in this step. An ammonium hydroxide solution (0.5 M) was then added and mixed together for 5 min. The vials were closed and kept for gelation and aging. The former was observed in the next 2 hours and the obtained gels were kept for aging

for one day at room temperature. After this period, the wet alcogels were either used directly in the adsorption experiments or dried under supercritical carbon dioxide ($T_c$ = 31.1 °C; $P_c$ = 73.7 bar) to obtain the silica aerogels.

This last step was preceded by a solvent exchange different from what was explained in previous sections, to ensure complete template removal. An effective and simple solution was proposed to address that issue, where template removal could be achieved as part of the supercritical drying procedure. This technique has (to our knowledge) never been tried before. To that end, the acetone exchange step was preceded by another 24 h solvent exchange step, with a solvent possessing very high miscibility with the template, and also acceptable miscibility with acetone. For caffeine, chloroform was chosen for this purpose, whereas for 2-naphthol, THF was chosen. The procedure became: after the 24 h aging period, the solids were placed in vials containing 30 mL of chloroform for caffeine imprinted gels or 30 mL of THF for 2-naphthol imprinted gels and placed under shaking at 120 rpm. To ensure maximum removal of template, five exchanges with the extracting solvent were performed within this 24 h period, where the gels would be removed from the vials and placed in others containing a new 30 mL chloroform/THF. After that, they would be placed in vials containing 30 mL of acetone, also under shaking at 120 rpm. Three exchanges were performed in acetone within that period of 24 h, similarly to what was just described. In a final step, the gels were $CO_2$ supercritically dried to become aerogels.

This modification proved to be a big success, as none of FTIR, HPLC, UV-VIS or fluorescence measurements were able to detect the slightest trace of template, enabling us to say with confidence that more than 99.9% of our template molecule was removed, without any harm done to the final structure of the aerogels. This supercritical

drying method was subsequently used for all molecularly-imprinted gels discussed in later sections. It is worth to mention that the solvent exchange procedure was followed for the molecularly-imprinted silica alcogels as well with the exception of the final supercritical drying step, to ensure complete template removal on one hand, and identical experimental conditions for the sake of consistency on the other.

The final molar ratios $Si(OR)_4$:Solvent:$H_2O$:HCl:$NH_3$ were $1:12:6:3\times10^{-3}:6\times10^{-3}$ for the gels where TMOS or TEOS were used alone as silicon precursors, whereas the ratios $Si(OR)_4$:R''$Si(OR')_3$:Solvent:$H_2O$:HCl:$NH_3$ were $0.8:0.2:12:6:3\times10^{-3}:6\times10^{-3}$ for the other gels, and the ratios $Si(OR)_4$:R''$Si(OR')_3$:Caffeine/2-naphthol:Solvent:$H_2O$:HCl:$NH_3$ were $0.8:0.2:0.075:12:6:3\times10^{-3}:6\times10^{-3}$ for imprinted with caffeine/2-naphthol as template molecules.

**B. Characterization of silica sol-gel materials for adsorption**

In an attempt to further understand the physico-chemical properties of the prepared silica alcogels and aerogels, complete structural and textural characterizations were performed on them. This section deals with both surface modified gels for the adsorption of methylene blue (discussed in chapter III) and molecular imprinted gels for selective adsorption (discussed in chapter IV). All the materials presented in table 2.1 were tested in adsorption of methylene blue, with some of them found to have a low impact on this work, while others clearly standing out. For that reason, characterization was performed on these top alcogels and aerogels: M2, M2'', M3, E1', E2, E2', E2'', E3 and E3''. The material used for molecular-imprinting was M2.

The aerogels were used in the characterization without further modifications after the supercritical drying step, whereas the alcogels were first soaked in liquid nitrogen twice for 10 min then freeze-dried for 24 h, in order to freeze the solvent contained within. The structural characterization of the silica gels was performed using a Thermo Nicolet 4700 Fourier Transform Infrared Spectrometer equipped with a Class 1 Laser. The measurements were performed in the 4000 to 400 $cm^{-1}$ range and using the transmission KBr pellet technique. Surface characterization was carried out using a Tescan Scanning Electron Microscope at high voltage of 30 kV after sputter-coating the samples with a thin layer of gold.

### *1. Surface-functionalized silica gels for methylene blue adsorption*

a. FTIR spectroscopy of surface-functionalized alcogels and aerogels

The FTIR spectra performed for phenyl-functionalized and non-functionalized silica alcogels and aerogels reflect a noticeable difference attributed to the existence of phenyl groups in the solid network. Regardless of the initial combination of precursors, the FTIR spectra reveal the same functional groups (for surface-functionalized and non-functionalized), which means that the drying technique does not affect the structure of the material.

**Table 2.2.** Characteristic vibration frequencies ($cm^{-1}$) in FTIR spectra of different synthesized non-functionalized and phenyl-functionalized silica aerogels.

| Non Functionalized gels | Phenyl-Functionalized gels | Type of vibration | Structural Unit |
|---|---|---|---|
| 3460 | 3440 | O−H and SiO−H | H−O−H…$H_2O$ and ≡SiO−H…$H_2O$ |
| 2910 | 2900 | $\nu_s$C−H | $-CH_3$ |
| 2840 | 2830 | $\nu_{as}$C−H | $-CH_2$ |
| 1630 | 1630 | $\delta$H−O−H | H−O−H |
| | 1420 | $\nu$C=C + $\delta$C−H in plane $2\nu$Si−C | Si−Ph |
| ~1200 | 1130 | $\nu_{as}$Si−O−Si (LO mode) | ≡Si−O−Si≡ |
| 1070 | 1070 | $\nu_{as}$Si−O−Si (TO mode) | ≡Si−O−Si≡ |
| 951 | 947 | $\nu_\beta$Si−O | ≡Si−O |
| 789 | 785 | $\nu_s$Si−O | ≡Si−O−Si≡ |
| | 739 | $\omega_{\delta,\gamma}$C−H | Si−Ph |
| | 696 | $\Phi$C−H | Si−Ph |
| 531 | 544 | $\nu$Si−O | $SiO_2$ defects |
| | ~476 | $\Phi$C−H | Si−Ph |
| 457 | 450 | $\delta$O−Si−O | −O−Si−O− |

Spectra of selected alcogels and aerogels are presented in figure 2.2. Table 2.2 shows the vibration frequencies obtained for both categories of aerogels where characteristic peaks of surface phenyl groups appear for functionalized samples in contrast to the non-functionalized ones [129]. This indicates the successful surface phenyl-functionalization whenever phenyltrialkoxysilane precursors are used in the synthesis. Characteristic vibrations corresponding to the bulk siliceous structure do appear for both categories without any noticeable difference.

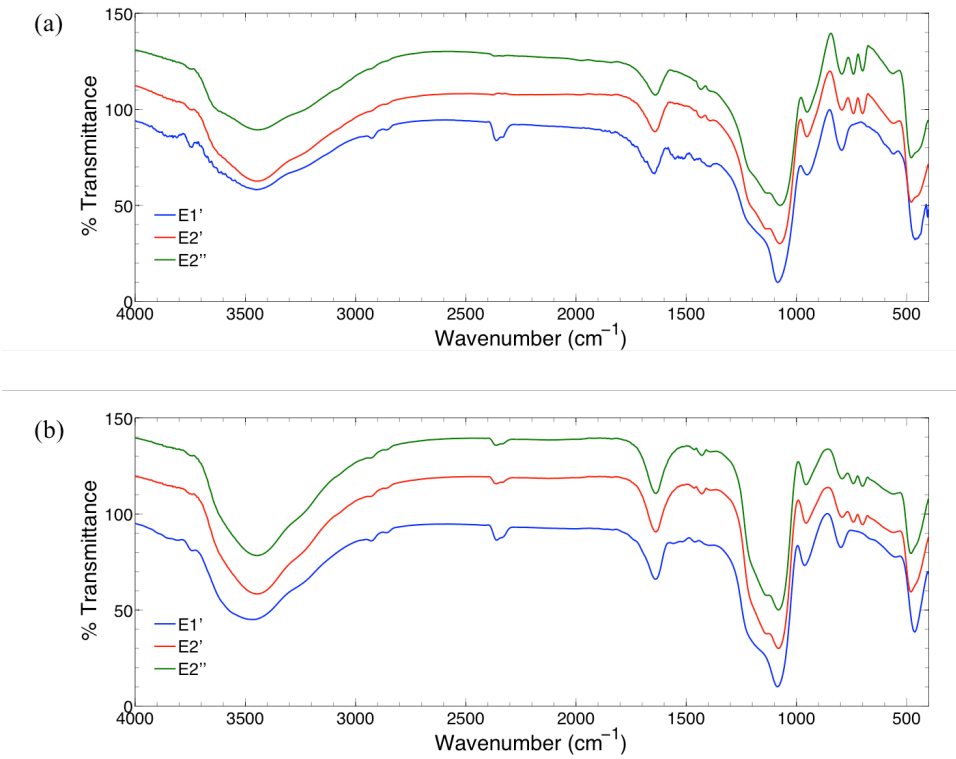


**Figure 2.2.** FTIR spectra in 1% KBR of E1', E2' and E2'' (a) alcogels and (b) aerogels with E1' serving as a non-functionalized reference.

b. SEM of surface-functionalized alcogels and aerogels

Scanning electron microscopy (SEM) micrographs reveal the porous structure of the various phenyl-modified aerogels where silica aggregates and large interconnected pores appear. The micrographs clearly show a "spongy" porous structured material, confirming the high porosity of obtained silica aerogels. SEM micrographs obtained for a representative aerogel are shown in figure 2.3. The alcogels revealed identical morphology by SEM to aerogels, indicating that freeze-drying the solvent within their pores does not affect the surface properties.

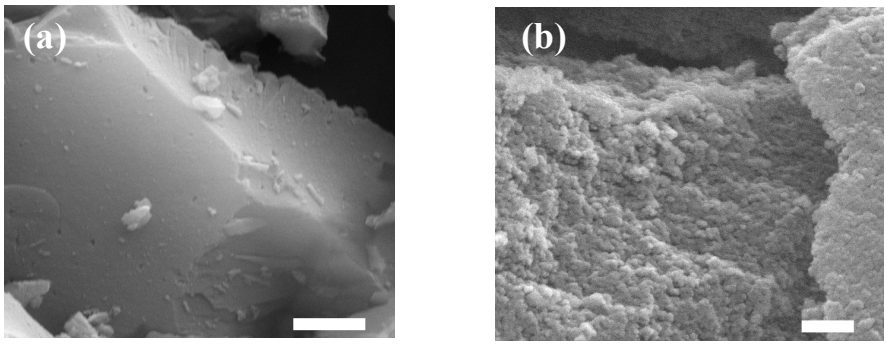


**Figure 2.3.** SEM images of TEOS-PhTMS aerogel synthesized in acetonitrile solvent at different resolutions: (a) 10 μm and (b) 200 nm.

### *2. Molecularly-imprinted silica gels*

Characterization of the molecularly-imprinted materials was limited to FTIR spectroscopy for gels imprinted with caffeine, and comparison with a caffeine reference peak, to check for template removal. Work is still under investigation to completely characterize these materials through porosity and surface area measurements, SEM/EDX, and TGA, but will not be presented due to lack of sufficient data at this point.

a. FTIR spectroscopy of molecularly-imprinted silica gels

FTIR spectra of molecularly-imprinted and non-imprinted TMOS alcogels and aerogels clearly reflect the differences in their structure. A reference caffeine FTIR spectrum is also presented in figure 2.4. The alcogels' spectra contain peaks assignable to their template molecules, mainly at 2750 $cm^{-1}$, ≈ 2900 $cm^{-1}$ (barely visible in figure 2.5), ≈ 1500 $cm^{-1}$, in the region of 700 $cm^{-1}$, at 1650 and 1700 $cm^{-1}$. The FTIR spectra of the aerogels do not show these peaks assignable to caffeine (figure 2.5). This indicates that the template molecule was successfully removed from the gel. Later measurements

on HPLC also show no caffeine leakage, thus confirming this statement, and will be discussed in chapter IV.

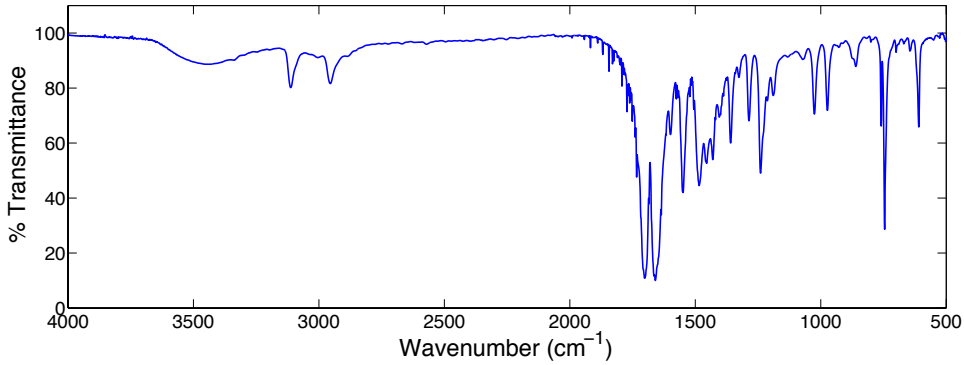


**Figure 2.4.** FTIR spectrum of caffeine in 1% KBR.

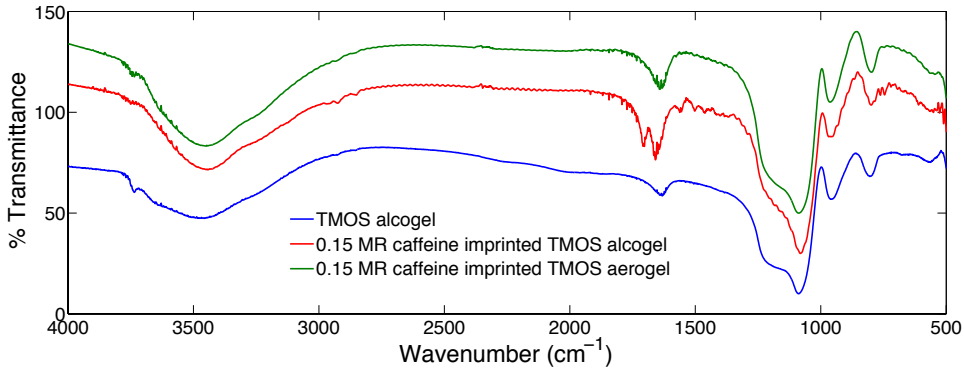


**Figure 2.5.** FTIR spectra in 1% KBR of TMOS alcogel; 0.15 MR caffeine imprinted TMOS alcogel and 0.15 MR caffeine imprinted TMOS aerogel.

## C. Conclusion

A complete and detailed overview of the synthesis of surface-functionalized and molecularly-imprinted silica alcogels and aerogels was presented, as well as full characterization of the obtained solid-state materials: FTIR spectroscopy was performed

to investigate their chemical structure, and SEM was carried out to elucidate surface properties. These techniques revealed that surface functionalization proved to be successful, adding surface functional groups without altering the core structure of the gel. Moreover, in the cases where molecular imprinting was involved, results showed that the template material was completely removed in the final structure of the gel, with no alterations to its core structure.

# CHAPTER III

# ADSORPTION OF METHYLENE BLUE ONTO SURFACE-MODIFIED SILICA SOL-GEL MATERIALS

In this chapter, a full study on surface modified silica aerogels for the removal of methylene blue from water via adsorption will be presented and discussed.

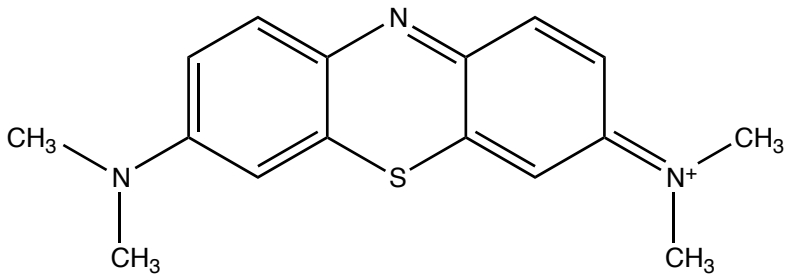


**Figure 3.1.** Chemical structure of methylene blue.

Methylene blue, whose structure is shown in figure 3.1, was chosen as the dye to be tested because it is one of the many dyes causing a problem for Lebanon's natural waters.

## A. Experimental description

All adsorption experiments were performed in glass vials under shaking in a Julabo SW 23 controlled-temperature water bath operating at 160 rpm. In a typical adsorption experiment, an initial amount of adsorbent was dropped in 30 mL of an

aqueous 15 mg/L (46 μM) methylene blue dye solution, at set pH and temperature. Aliquots were carefully withdrawn at pre-determined time intervals over 4 h, and the MB concentration was determined by measuring the absorbance of the solution at the maximum absorption wavelength (λ = 664 nm) using a Thermo Scientific Evolution 300 UV/VIS/NIR spectrophotometer. The aliquots were centrifuged whenever small gel particles were present using a Thermo Scientific Heraeus Pico 17 centrifuge. The amount of adsorbed dye on the solids was calculated according to the following equation:

$$q_e = \frac{C_o - C_e}{m} V \tag{3.1}$$

where $q_e$ is the amount of dye adsorbed at equilibrium (mg/g), $C_o$ and $C_e$ are the initial and equilibrium liquid-phase concentrations of dye (mg/L) respectively, $V$ is the volume of solution (L) and $m$ is the amount of adsorbent (g).

Because the exact weighing of the alcogels was almost impossible due to the existence of the solvent within the pores, the alcogels were dropped whole in the solution and specific mass measurements were not performed on them. These materials were used as a stepping-stone to pinpoint the best precursor/co-precursor/solvent combination for later more specific work on aerogels. These latter were weighed accurately and their masses were recorded before their use as adsorbents of dye from aqueous media.

The effect on adsorption of silicon precursors, solvent used in the synthesis of the gels, and temperature was studied. The effect of pH was investigated after the adjustment of the pH of the methylene blue solutions using dilute $H_2SO_4$ and $NH_4OH$ solutions and a Corning Pinnacle 542 pH conductivity meter with a combined pH electrode. In order to evaluate the effect of the size of the adsorbing material on its

efficiency, crushed and uncrushed adsorbents were compared. The initial dye concentration was studied in the range between 1 and 300 ppm, and the dosage of the silica aerogels was investigated in the 20 to 600 mg range.

### B. Effect of pH and silicon precursors on adsorption

The UV-Vis spectra of methylene blue aqueous solutions were found to be different at various pHs as shown in Figure 3.2.

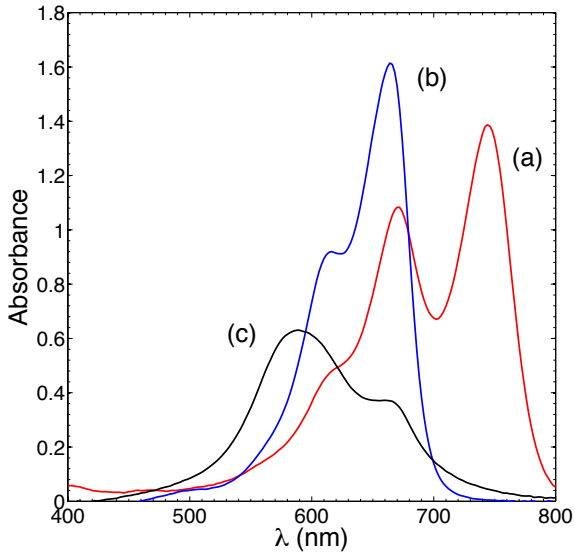


**Figure 3.2.** UV-VIS spectra of 10 mg/L (31 μM) methylene blue at (a) pH = 1; (b) pH between 2 and 10 and (c) pH greater than 10.

The correlation between the spectra obtained and reported characteristic peaks of methylene blue [130] shows that the protonated form $MBH^{2+}$ dominates at pH 1 whereas in the pH range between 2 and 10 the monomer $MB^{+}$ is dominant. At higher pHs, the dimer $(MB^{+})_2$ and trimer $(MB^{+})_3$ forms dominate. Accordingly, we selected the range between pH 2 and 10 to be used in this study as this is where the monomer form

of methylene blue dominates. The adsorption of the dye on the solid material was followed at 664 nm ($\lambda_{max}$).

Determining the effect of the surface functionalization of silica gels and the variation of the silicon precursors on the adsorption of methylene blue has been studied. Three different gels made according to the procedure described in previous sections were synthesized to understand the correlation between MB adsorption and surface functionalization of the silica gels in which TEOS was solely used as silicon precursor or coupled with VTES or PhTES as co-precursors. Methanol was used for all gels as synthesis solvent. A study of the pH effect on the adsorption of the dye onto those three alcogels was conducted where the pH was varied between 2 and 10. The gels (i.e. adsorbents) were dropped in glass vials containing 30 mL of 15 mg/L (46 μM) methylene blue solution, shaking at a controlled temperature of 30°C and 160 rpm, for 4 h. Aliquots were quantified in UV-VIS spectroscopy.

The difference between alcogels and xerogels was investigated, where alcogels were used after aging at room temperature for 48 h whereas the xerogels were left for 10 days before use resulting in denser, shrunk, glass-like solids. As expected, the xerogels showed very little adsorptive capacity with respect to the alcogels due to the decrease in their porosity; therefore studying the adsorption capacity of the xerogels was found not to be of an interest. The UV-Vis measurements show an increasing percent removal of the dye after 4 hours with increasing pH, with a maximum adsorption at pH 8 and 9 (figure 3.3). The surface functionalization of the silica alcogels shows also a crucial impact on the adsorptive capacity with the TEOS-PhTES alcogel being the best at almost all pHs, with clear maxima at pH 8 and 9.

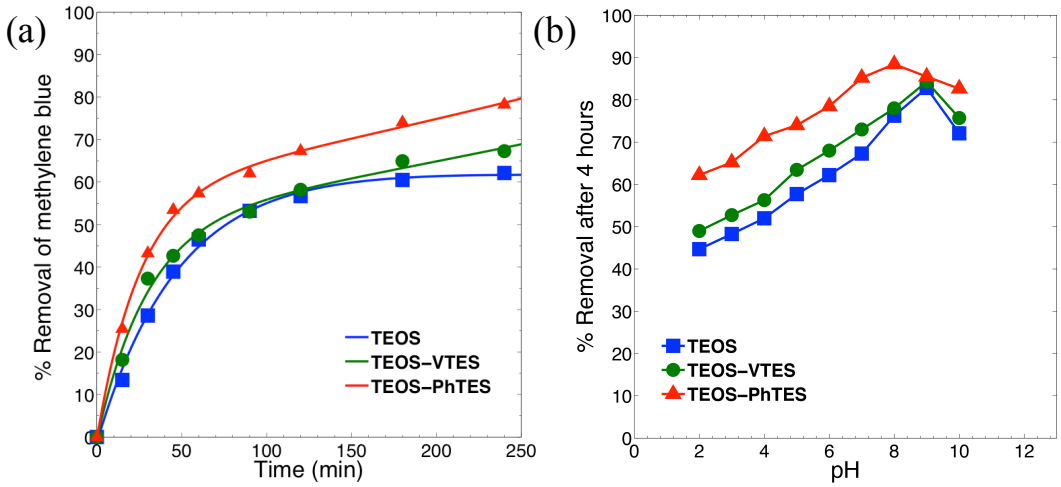


**Figure 3.3.** (a) %Removal of methylene blue as a function of time for TEOS, TESO-VTES and TEOS-PhTES alcogels in methanol at pH = 6. (b) Effect of pH on adsorption of methylene blue onto silica alcogels. Initial MB concentration = 15 mg/L (46 μM); contact time = 4 h; solution volume = 30 mL.

The difference in the adsorption capacity at different pHs can easily be attributed to the surface charge of the adsorbent. The point of zero charge (PZC) of silica is around 2.5 [131], meaning that for lower pH it exhibits a positive zeta potential resulting in a positively charged surface of the adsorbent. This has a negative impact on the dye adsorption due to the electrostatic repulsion between the adsorbent surface and the positively charged methylene blue monomer $MB^+$. Following the same reasoning, the adsorption capacity of the solids should be higher with an increase in the pH due to the abundance of negative surface charges on the adsorbent which favors the electrostatic attraction between the negatively charged $Si\text{-}O^-$ surface groups and the positively charged $MB^+$ dye monomer.

On the other hand, the difference in the adsorption capacities of the three different silica alcogels can be explained by the difference in the intermolecular forces between the different surface groups and the dye monomer.

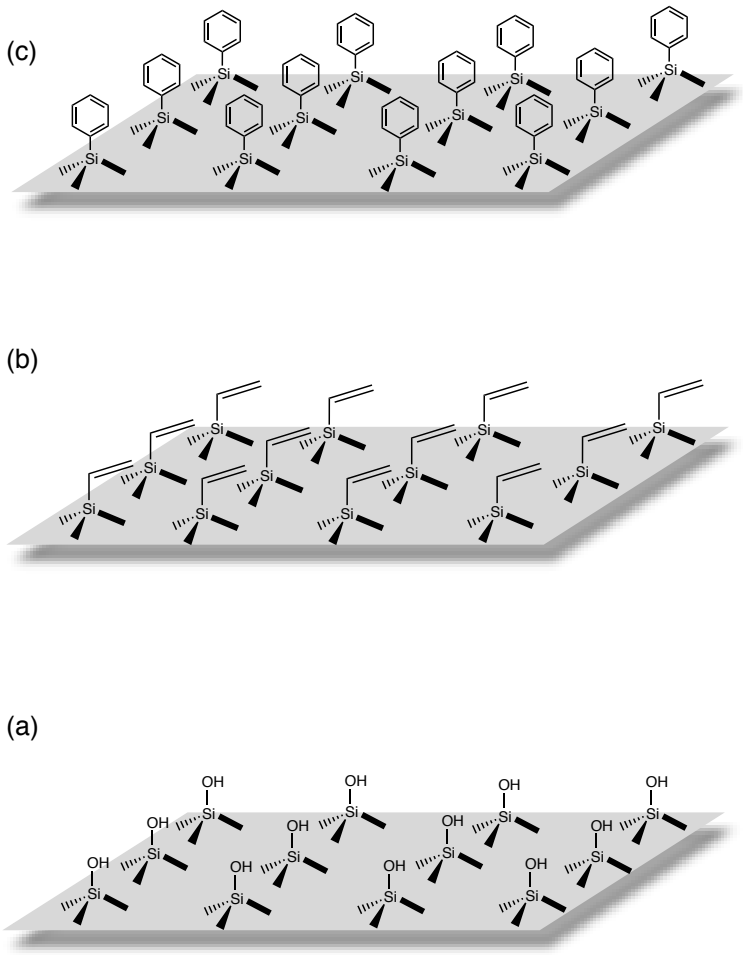


**Figure 3.4.** Surface chemistry of the silica gels: (a) TEOS used only as silica precursor, (b) TEOS-VTES co-precursors, and (c) TEOS-PhTES co-precursors.

Figure 3.4 shows the surface of the gels, where TEOS is solely used as silicon precursor (a), or coupled with VTES (b) and PhTES (c) as co-precursors. When TEOS alcogels are used in adsorption, the surface silanol groups (Si-OH) make for a strong hydrogen bonding between the gel and the $MB^+$ dye monomer, whereas in the case of TEOS-VTES alcogels, the presence of vinyl surface groups in addition to silanols allow

for an additional good π electrons attractions and thus a superior attraction between the dye molecules and the alcogel surface groups. The aromatic rings on the surface of phenyl-functionalized gels (TEOS-PhTES) offer a superior degree of delocalization due to the π-π stacking of the phenyl surface groups and the aromatic rings of the dye molecule. Thus, comparing these three surface-dye interactions, the latest was expected to show the highest adsorption capacity; this was confirmed experimentally where we found the phenyl-functionalized alcogel the best in the whole pH range and the non-functionalized solid revealing the weakest adsorption capacity. Based on these results, phenyl-functionalized gels were selected for adsorption in the following sections in this study.

**C. Effect of synthesis solvent**

In order to explore the full potential of the phenyl co-precursor, alcogels with combinations of TMOS, TEOS, PhTMS and PhTES as precursors were synthesized. Along with these combinations, the solvent used in the synthesis of the gel was also varied, where methanol, acetone and acetonitrile were explored. All the gels thus synthesized are regrouped and labeled in table 2.1. Adsorption experiments were conducted on each of the aforementioned 18 alcogels at pHs between 4 and 10 in order to reassert the pH effect in combination with the different solvents and precursor combinations, as a first step for later work on aerogels. The pH range was chosen so that the methylene blue will be in its cationic monomeric form ($MB^+$) and the silica solids above their PZC.

The solvent was found to play a crucial role in the resulting adsorptive capacities of the gels (figure 3.5) implying a direct correlation between the surface

properties of the materials and the polarity of the used solvent. Aprotic acetonitrile is known to be the most polar of the three solvents being studied, followed closely by the protic methanol and aprotic acetone [132]. These characteristics play an important role in the synthesis process, having an impact on the precursors' hydrolysis and condensation rate constants $k_H$ and $k_C$, respectively [3, 4]. During the hydrolysis, it is known that $k_H$ increases linearly with the concentration of $[H^+]$ in the medium [53]. It was also shown through $^{29}Si$ NMR that the solvent has a secondary important effect on the hydrolysis rate constant, being the highest in acetonitrile, then in order of decreasing $k_H$, methanol, dimethylformamide, dioxane, and formamide [53].

The solvent nature does not play a role in the hydrolysis step alone, but it also affects the sol condensation and gelation, although separating the effect of the solvent from that of the alkoxy precursor in that process rapidly becomes a very challenging task. However, scientists seem to agree that a trend exists dictating that the larger the solvent molecule size is, the longer is the gelation time [4]. Brinker and Scherer [3] argue that polar protic solvents, such as methanol in the current work, offer the possibility of hydrogen bonding to the anionic nucleophile $SiO^-$ involved in the condensation reaction thus making it less nucleophilic. This is not the case for polar aprotic solvents such as acetone and acetonitrile. However, due to their relatively high polarity, this nucleophile is stabilized with respect to the activated complex, which results in slowing down the reaction.

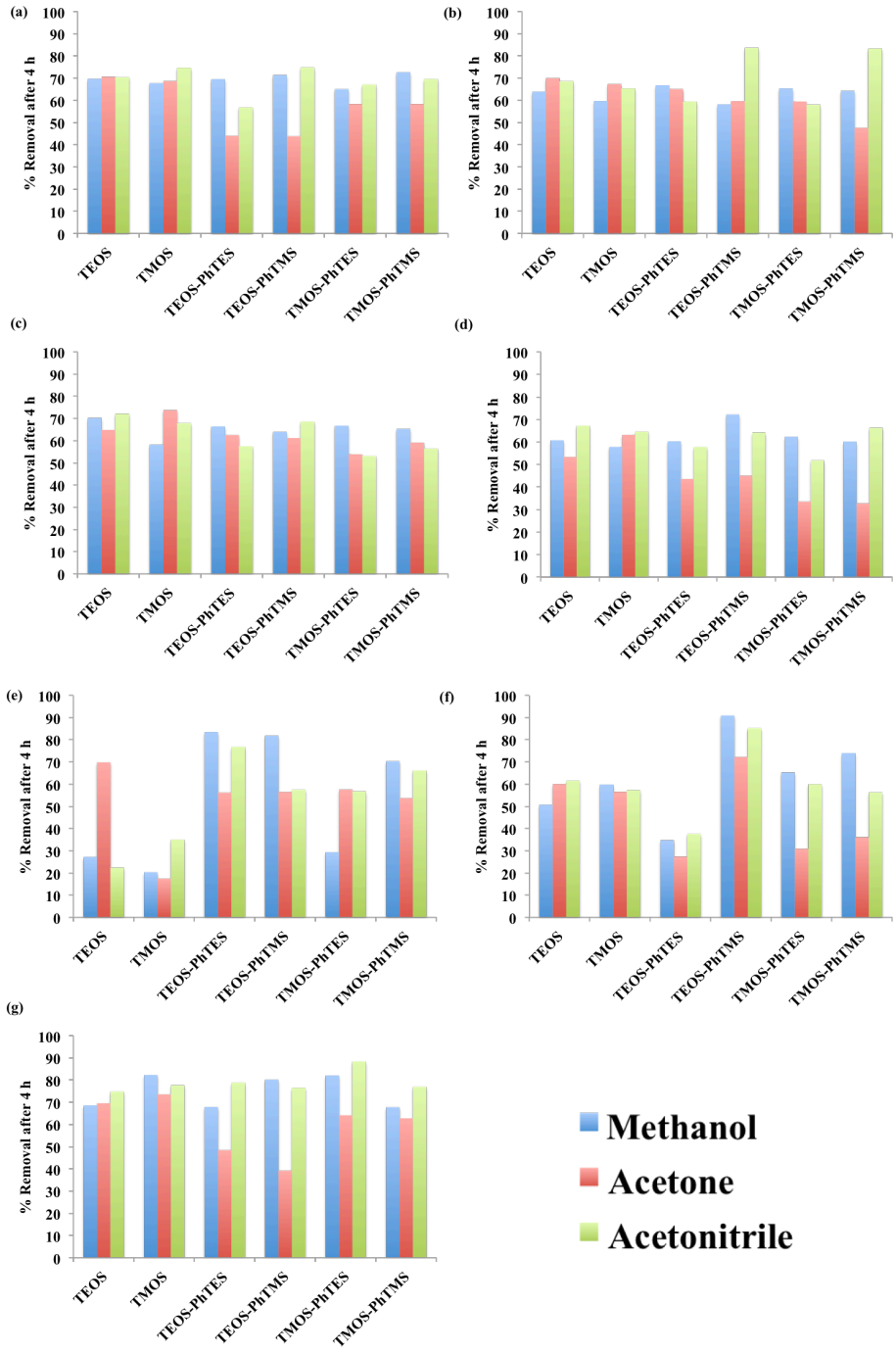


**Figure 3.5.** % Removal of methylene blue after 4 h for alcogels synthesized in different solvents with different silica precursors, at different pHs: (a) pH = 4; (b) pH = 5; (c) pH = 6; (d) pH = 7; (e) pH = 8; (f) pH = 9 and (g) pH = 10. Initial MB concentration = 15 mg/L (46 μM); contact time = 4 h; solution volume = 30 mL.

After a thorough analysis of the significant amount of results obtained, the study was narrowed down to nine silicon precursors-solvent combinations to be tested as aerogels in adsorption at the best 2 pHs. The selection was made based on the results obtained at the best two pHs (8 and 9) where we selected the best nine solids that exhibit the highest percent adsorption after 4 h of contact time between the adsorbent and adsorbate. The selected aerogels are: TMOS-PhTMS in methanol (M2) and acetonitrile (M2"), TMOS-PhTES in methanol (M3), TEOS in acetone (E1'), TEOS-PhTMS in methanol (E2), acetone (E2'), and acetonitrile (E2"), TEOS-PhTES in methanol (E3) and in acetonitrile (E3").

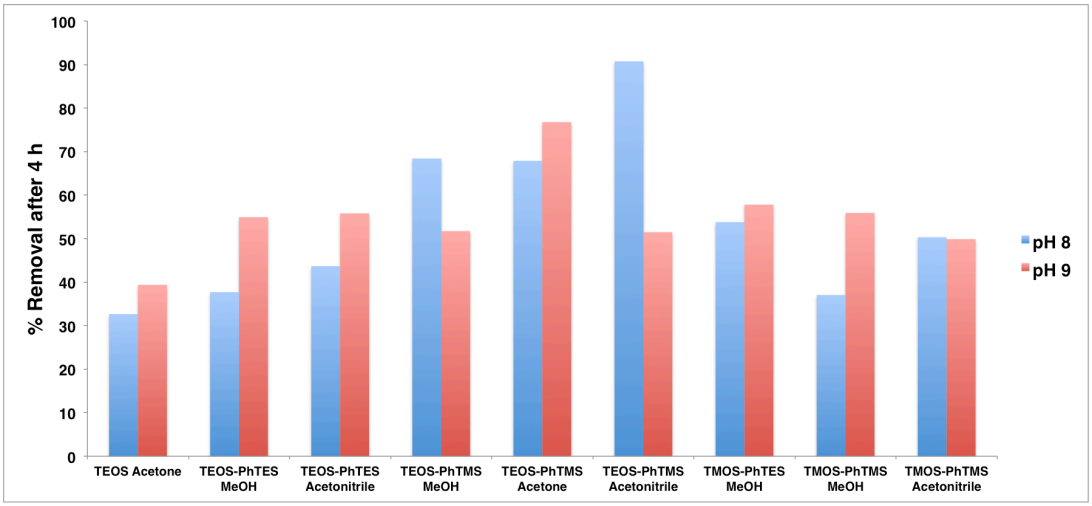


**Figure 3.6.** Comparison of the %Adsorption after 4 hours of selected silica aerogels at pH 8 and 9. Initial aerogel dose = 100 mg; initial MB concentration = 15 mg/L (46 µM); contact time = 4 h; solution volume = 30 mL.

The difference in the adsorptive capacity of the studied aerogels (figure 3.6) indicates that the synthesis solvent still plays a crucial role in the adsorption process, even after it has been completely removed during the $CO_2$ supercritical drying step. The comparison of the obtained adsorption results revealed one silicon precursors

combination (TEOS-PhTMS) to be the best at both pHs, where the synthesis solvent was acetonitrile for the best aerogels at pH 8 (E2") whereas acetone was used in the synthesis of the aerogel having the highest adsorption capacity at pH 9 (E2').

**D. Effect of gel particle size on adsorption**

The effect of gel particle size on adsorption was studied for alcogels and aerogels alike. To that end, TEOS-PhTMS in acetonitrile (E2") and TEOS-PhTMS in acetone (E2') were prepared as alcogels and aerogels to be used in adsorption. The first adsorbent was tested at pH 8 whereas the second was used at pH 9 according to the results reported in the previous sections.

To study the effect of the particle size of the adsorbent (either alcogel or aerogel) on its adsorptive capacity, the gels were either dropped whole in the solution or crushed into small pieces (powder in the case of aerogels). The masses of the adsorbents were kept constant in the adsorption experiments where 100 mg of the aerogels were used. However since it is extremely difficult to get an accurate mass reading for the alcogel due to the large amount of solvent and water present in the gel matrix, the full amount of gel prepared in one propylene vial was used per experiment.

The results showed that particle size has a very pronounced effect on the adsorptive capacity of both alcogels and aerogels (figure 3.7), with the effect being much more noticeable when aerogels are used. Crushing the gel affects the kinetics of the adsorption process (as seen in the measurement taken after 5 min), making it significantly faster as well as the final adsorptive capacity of the gel at equilibrium (as seen in the measurement taken after 240 min).

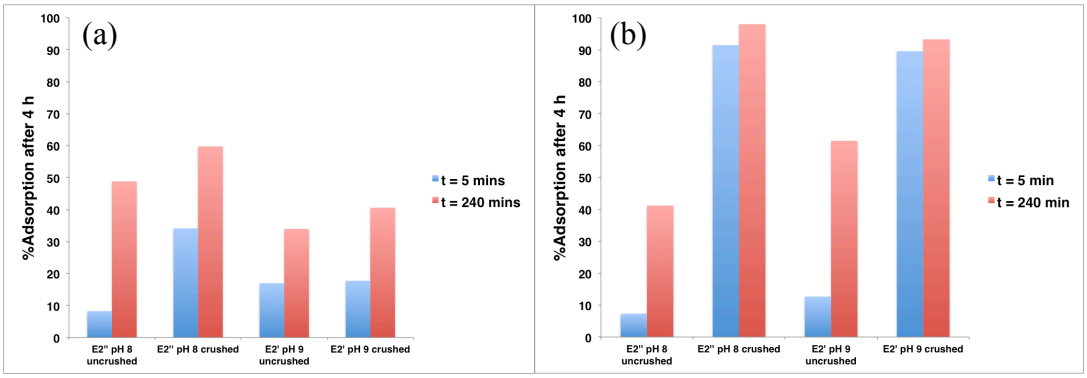


**Figure 3.7.** Comparison of the %Adsorption of E2'' at pH 8 and E2' at pH 9 crushed and uncrushed (a) alcogels and (b) aerogels at t = 5 min and t = 240 min. Initial aerogel dose = 100 mg; initial MB concentration = 15 mg/L (46 µM); contact time = 4 h; solution volume = 30 mL.

This behavior is due to the drastic increase of the contact surface area in the case of crushed adsorbents making the adsorption sites more easily accessible by the methylene blue molecules; a very simple yet very important observation. The comparison of the adsorption capacities of crushed aerogels to that of crushed alcogels revealed a much higher adsorption for the former adsorbents. This can be due to the easier diffusion of the dye molecules within the free pores of the aerogel whereas the diffusion is not easy when the pores are filled with the solvent and water used in the alcogel synthesis. Accordingly, aerogels after being crushed were selected to conduct the adsorption experiments in the following steps.

### E. Effect of initial methylene blue concentration

The methylene blue adsorption capacity of the best two aforementioned aerogels has been studied as a function of the dye initial concentration. The methylene blue solution concentration was adjusted between 1 and 300 ppm, and the pH to optimal conditions (8 for E2" aerogel and 9 for E2' aerogel), the temperature was set at 30°C,

and the methylene blue adsorption was followed at predefined time intervals. The MB concentrations in the solutions after 4h of contact time are used in this section as considered at equilibrium. It is worth mentioning that the studied methylene blue concentrations were below the dye solubility limit in water, which implies that the decrease in dye concentration over time is due solely to its adsorption on the surface of the gel, and not to the recrystallization of the MB salt.

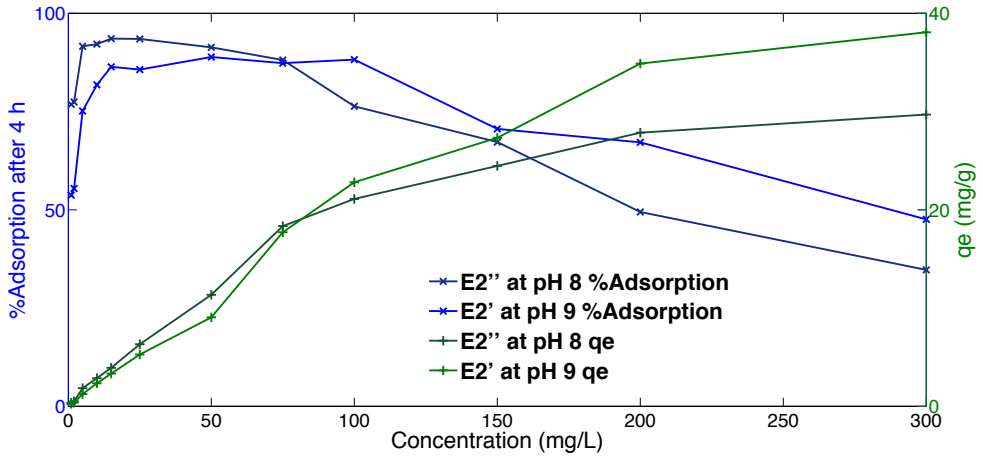


**Figure 3.8.** Plot of the effect of initial concentration variation, relating both the equilibrium adsorptive capacity (right y-axis, in mg/g) and the %Adsorption after 4 hours (left y-axis) to the initial concentration of methylene blue solution (mg/L) for E2'' at pH 8 and E2' at pH 9 aerogels. Initial aerogel dose = 100 mg; contact time = 4 h; solution volume = 30 mL.

Figure 3.8 shows the change of percent adsorption of methylene blue at equilibrium while increasing the initial dye concentration, as well as the adsorptive capacity $q_e$ of both aerogels. An interesting observation is that even though the E2" aerogel at pH 8 presents a higher percent adsorption especially at relatively low concentrations, the equilibrium adsorption capacity $q_e$ has been found to be very similar for both aerogels at relatively low concentrations, whereas for concentrations greater

than 100 ppm, a clear detachment of the two curves can be observed. At 300 ppm for instance, the difference is even more pronounced with E2' aerogel at pH 9 showing a much higher adsorptive capacity than E2" aerogel at pH 8 (39.1 and 29.7 mg/g, respectively).

**F. Methylene blue adsorption isotherms**

Collected adsorption data at methylene blue concentrations ranging between 1 and 300 ppm (section E) were fitted with seven adsorption models: Langmuir [133], Freundlich [134], Temkin [135], Dubinin-Radushkevich [136], Redlich-Peterson [137], Toth [138] and Sips [139, 140] isotherm models. The results are presented below [131, 141].

The Langmuir isotherm equation is represented by

$$q_e = \frac{q_{\max} K_L C_e}{1 + K_L C_e} \tag{3.2}$$

where $q_{\max}$ is the monolayer adsorption capacity of the adsorbent (mg/g) and $K_L$ is the Langmuir equilibrium constant (L/mg).

The Freundlich isotherm is represented by

$$q_e = K_F C_e^{1/n} \tag{3.3}$$

where $n$ and $K_F$ are the heterogeneity factor (generally greater than 1 and an indication of the linearity of the adsorption isotherm; the greater the value the more non-linear the isotherm and the greater the heterogeneity of the system) and the Freundlich constant (L/g) respectively, both temperature dependent.

The Temkin equation is represented by

$$q_e = \frac{RT}{b_T} \ln C_e + \frac{RT}{b_T} \ln K_T \tag{3.4}$$

where $R$ is the universal gas constant (8.3145 J/mol.K), $T$ is the absolute temperature, $b_T$ is the variation of the adsorption energy (J/mol) and $K_T$ is the equilibrium binding constant (L/g).

Similar to the Langmuir isotherm but without assuming a homogeneous surface or constant sorption potential, the Dubinin-Radushkevich (D-R) equilibrium isotherm is represented by the following equation

$$q_e = q_{\max} \exp(-\beta \varepsilon^2) \tag{3.5}$$

where $q_{\max}$ is the D-R monolayer capacity (mg/g), $\beta$ is a constant related to the adsorption energy ($mol^2/kJ^2$), and $\varepsilon$ is the Polanyi potential related to the equilibrium concentration as follows:

$$\varepsilon = RT \ln(1 + \frac{1}{C_e}) \tag{3.6}$$

D-R isotherm allows for the determination of the mean free energy of adsorption ($E$, J/mol), which can be calculated according to the following relationship

$$E = \frac{1}{\sqrt{2\beta}} \tag{3.7}$$

A slightly more complex isotherm is the Redlich-Peterson (R-P) equilibrium isotherm that can be expressed as follows

$$q_e = \frac{K_R C_e}{1 + a_R C_e{}^{b_R}} \tag{3.8}$$

where $K_R$ and $a_R$ are Redlich-Peterson isotherm constants (L/g and $(L/mg)^{bR}$ respectively) and $b_R$ is the R-P isotherm exponent. It is worth mentioning that this isotherm is a hybrid model featuring Langmuir and Freundlich isotherms. At low

concentrations, the Redlich-Peterson isotherm approximates the ideal Langmuir model, while at high concentration it behaves similarly to the Freundlich isotherm [142].

Derived from potential theory, the Toth isotherm can be expressed by

$$q_e = \frac{K_t C_e}{(a_t + C_e)^{1/t}} \tag{3.9}$$

where $K_t$ (L/g) and $a_t$ are Toth isotherm constants and $t$ is the Toth isotherm exponent. The main premise of that equilibrium isotherm is that it assumes that most sites have a sorption energy less than the mean value [141].

The last isotherm that the experimental data were fitted with was the generalized Sips equilibrium isotherm, expressed by the following equation:

$$q_e = \frac{q_{\max}(a_s C_e)^{n_s}}{1 + (a_s C_e)^{n_s}} \tag{3.10}$$

where $a_s$ is the Sips isotherm constant and $n_S$ is the Sips isotherm exponent.

The Langmuir, Freundlich, Temkin, Dubinin-Radushkevich, Redlich-Peterson, Toth and Sips isotherm constants were computed by fitting the experimental data with the corresponding model (figure 3.9). These constants as well as their non-linear correlation coefficients ($R^2$) are regrouped in table 3.1. The data comparison shows clearly that the three-parameter Sips equilibrium isotherm represents the best fit of the experimental results for both adsorbents. Theoretically calculated maximum monolayer capacities ($q_{\max}$) from Sips isotherm model were found to be 33.7 mg/g for E2" aerogel in a methylene blue solution at pH 8, and 49.2 mg/g for E2' aerogel in a pH 9 dye solution.

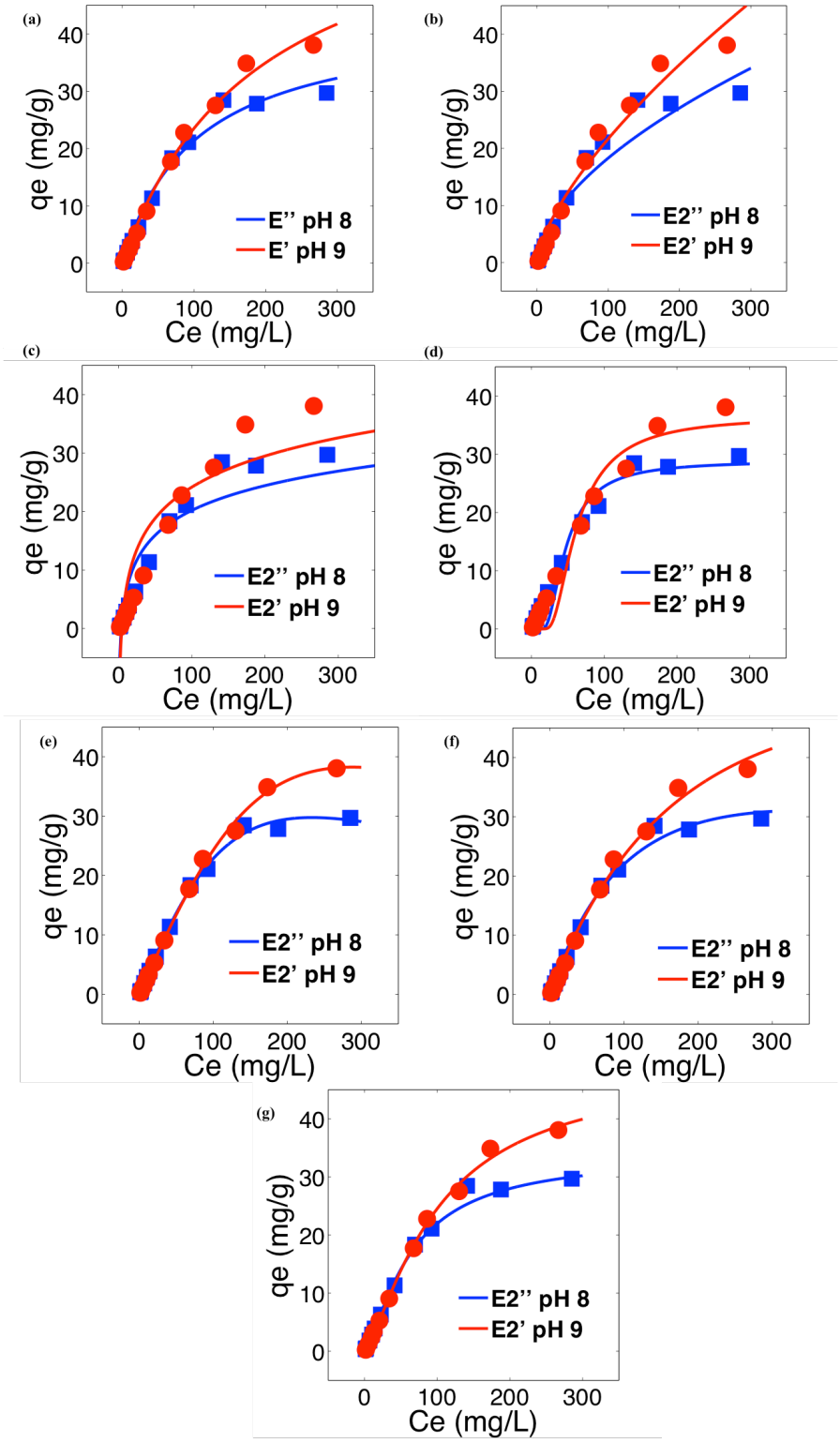


**Figure 3.9.** Langmuir (a), Freundlich (b), Temkin (c), Dubinin-Radushkevich (d), Redlich-Peterson (e), Toth (f) and Sips (g) isotherm plots for adsorption of methylene blue on E2'' at pH 8 and E2' at pH 9 aerogels. Initial aerogel dose = 100 mg; initial MB concentration = 1 - 300 mg/L (3 - 940 μM); contact time = 4 h; solution volume = 30 mL.

**Table 3.1.** Langmuir, Freundlich, Temkin, Dubinin-Radushkevich, Redlich-Peterson, Toth and Sips isotherm constants compiled for E2'' and E2' aerogels at pH 8 and 9 respectively.

| | Langmuir Isotherm | | | Freundlich Isotherm | | |
|---|---|---|---|---|---|---|
| | $q_{max}$ (mg/g) | $K_L$ (L/mg) | $R^2$ | *n* | $K_F$ (L/g) | $R^2$ |
| E2" aerogel pH 8 | 43.36 | 0.009723 | 0.984 | 1.781 | 1.443 | 0.938 |
| E2' aerogel pH 9 | 68.15 | 0.005269 | 0.992 | 1.475 | 0.9552 | 0.971 |

| | Temkin Isotherm | | | Dubinin-Radushkevich Isotherm | | | |
|---|---|---|---|---|---|---|---|
| | $b_T$ (J/mol) | $K_T$ (L/g) | $R^2$ | β ($mol^2/kJ^2$) | $q_{max}$ (mg/g) | E (kJ/mol) | $R^2$ |
| E2" aerogel pH 8 | 392 | 0.2677 | 0.887 | 0.0002628 | 28.86 | 43.62 | 0.953 |
| E2' aerogel pH 9 | 328.5 | 0.2343 | 0.854 | 0.0004606 | 36.52 | 32.95 | 0.949 |

| | Redlich-Peterson Isotherm | | | | Toth Isotherm | | | |
|---|---|---|---|---|---|---|---|---|
| | $K_R$ (L/g) | $a_R$ $(L/mg)^{bR}$ | $b_R$ | $R^2$ | $K_t$ (L/g) | $a_t$ | t | $R^2$ |
| E2" aerogel pH 8 | 0.2969 | 9.33E-05 | 1.754 | 0.987 | 9056 | 279.2 | 0.5588 | 0.991 |
| E2' aerogel pH 9 | 0.277 | 2.03E-05 | 1.922 | 0.988 | 2436 | 375.2 | 0.6665 | 0.994 |

| | Sips Isotherm | | | |
|---|---|---|---|---|
| | $q_{max}$ | $a_s$ | $n_s$ | $R^2$ |
| E2" aerogel pH 8 | 33.69 | 0.01641 | 1.47 | 0.994 |
| E2' aerogel pH 9 | 49.18 | 0.00997 | 1.337 | 0.997 |

## G. Effect of adsorbent dose

The effect of the quantity of aerogel used for adsorption was studied. Adsorbent masses ranged between 20 and 600 mg per experiment, and 15 mg/L (46 μM) methylene blue concentration was used. The pH was adjusted to the optimal 8 (for E2" aerogel) and 9 (for E2' aerogel) and the temperature was kept at 30°C. UV-VIS spectroscopic measurements showed that the maximum adsorption values after 4 hours were obtained at doses of 50 and 100 mg of adsorbent for both gels.

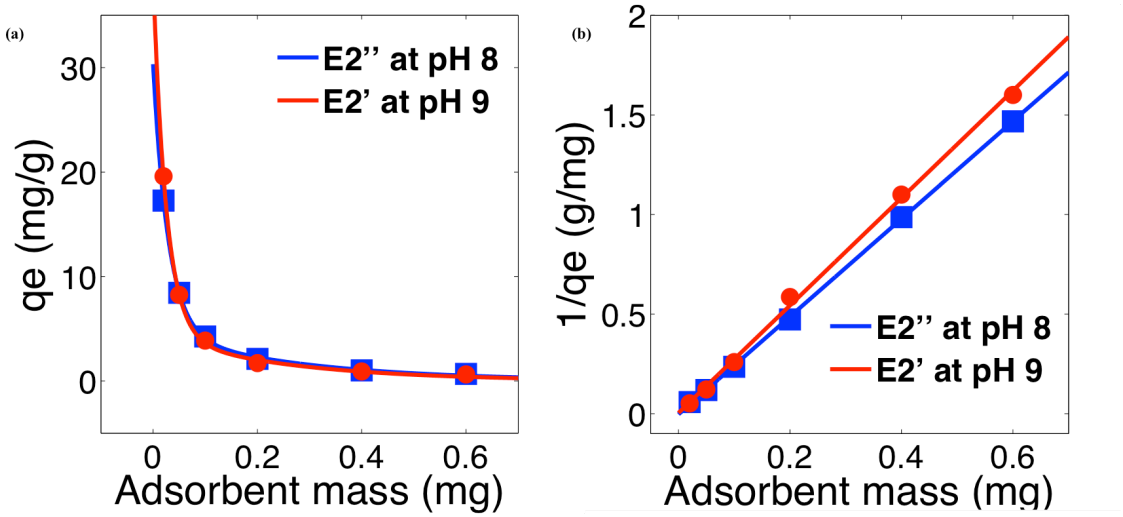


**Figure 3.10.** (a) Plot of $q_e$ vs $m$; (b) Plot of $1/q_e$ vs $m$ for E2'' at pH 8 and E2' at pH 9 aerogels. Initial aerogel dose = 20 – 600 mg; initial MB concentration = 15 mg/L (46 µM); contact time = 4 h; solution volume = 30 mL.

The plot of the relative amount of dye $q_e$ (in mg of dye per g of adsorbent) versus the quantity of adsorbent shows a decrease in $q_e$ as the quantity of adsorbent increases (figure 3.10a). $1/q_e$ versus adsorbent quantity gave a linear plot (figure 3.10b), which reveals that adsorption sites are available when large adsorbent quantities are used as well as when small quantities are used [94]. For instance, 50 mg of TEOS-PhTMS in acetonitrile at pH 8 and 50 mg of TEOS-PhTMS in acetone at pH 9 are able to remove 94 and 91% of methylene blue molecules existing in 30 mL of a 15 mg/L (46 µM) dye solution, respectively.

## H. Adsorption kinetics

The adsorption kinetics were studied in the 30-60°C temperature range. However, because the results obtained are similar, we selected to present only those

corresponding to the experiments performed at 30°C. The dye adsorption kinetics was monitored over 4 h and the experimental data were fitted to four kinetic models, namely first, second, pseudo-first, and pseudo-second orders.

The integrated first order rate equation is

$$C_t = C_0 e^{-k_1 t} \tag{3.11}$$

with $C_t$ being the methylene blue concentration (mg/L) at time $t$ (min), $C_0$ the initial methylene blue concentration (mg/L) and $k_1$ the first order rate constant ($min^{-1}$).

The integrated second order rate equation is:

$$\frac{1}{C_t} = \frac{1}{C_0} + k_2 t \tag{3.12}$$

with $k_2$ being the second order rate constant ($L.mg^{-1}.min^{-1}$).

The pseudo-first order rate equation can be expressed as

$$q_t = q_e(1 - e^{-k_1' t}) \tag{3.13}$$

where $q_e$ is the is the adsorption capacity of the silica aerogel at equilibrium (mg/g), $q_t$ is the amount of dye adsorbed (mg/g) at time $t$ (min) and $k_1'$ is the pseudo-first order rate constant ($min^{-1}$).

The pseudo-second order equation can be written as follows

$$q_t = \frac{k_2' q_e^{\,2} t}{1 + k_2' q_e t} \tag{3.14}$$

where $k_2'$ is the pseudo-second order rate constant ($g.mg^{-1}.min^{-1}$).

The linear fitting of the results to the first and second order models (figure 3.11), and the non-linear fitting to the pseudo-first and pseudo-second models (figure 3.12) indicate beyond the shadow of a doubt that the pseudo-second order model fits perfectly with the experimental data with correlation coefficients ($R^2$) greater than 0.9968. This result gives some insight into the adsorption mechanism, suggesting that

the adsorption depends on the adsorbate as well as the adsorbent, involving both chemisorption and physisorption processes [94, 143].

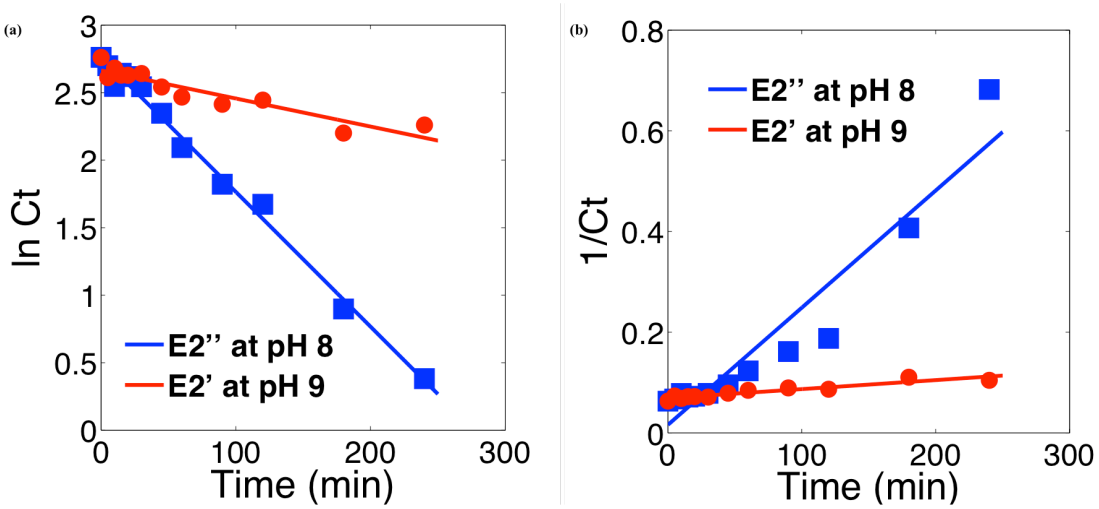


**Figure 3.11.** (a) Linear first order and (b) linear second order kinetics plots for adsorption of methylene blue by E2'' at pH 8 and E2' at pH 9 aerogels. Initial aerogel dose = 100 mg; initial MB concentration = 15 mg/L (46 μM); contact time = 4 h; solution volume = 30 mL.

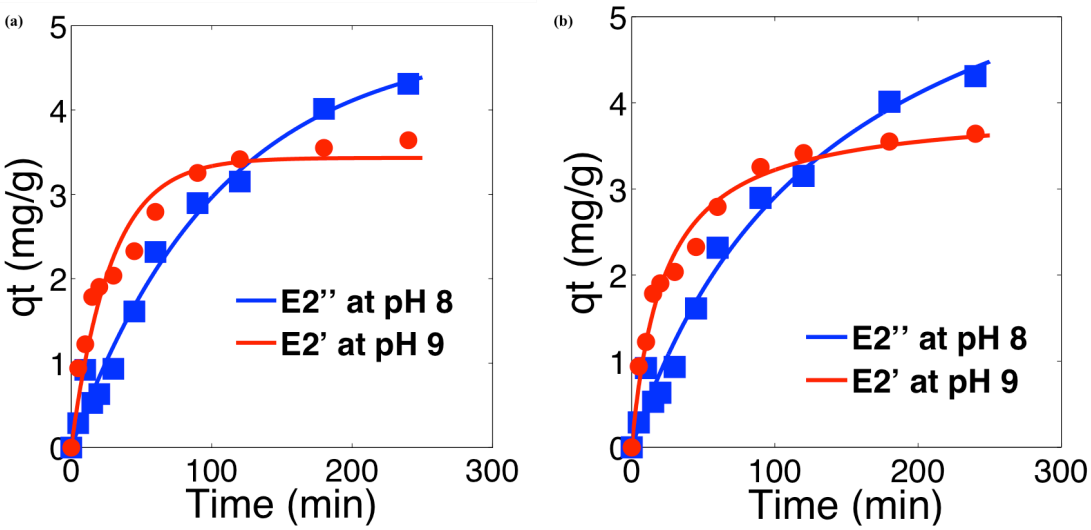


**Figure 3.12.** (a) Non-linear pseudo-first order and (b) non-linear pseudo-second order kinetics plots for adsorption of methylene blue by E2'' at pH 8 and E2' at pH 9 aerogels. Initial aerogel dose = 0.1000 g; initial MB concentration = 15 mg/L (46 μM); contact time = 4 h; solution volume = 30 mL.

## I. Effect of temperature

Adsorption experiments were performed at 4 different temperatures: 30, 40, 50 and 60°C in order to study the effect of temperature on the MB removal. The activation energy ($E_a$) for the adsorption of dye onto the surface of selected aerogels was calculated from the rate constants ($k_2$) obtained for the reactions performed at each temperature where 15 mg/L (46 µM) dye solutions were used. The Arrhenius equation was used for this purpose:

$$k = Ae^{-E_a/RT} \tag{3.15}$$

where $A$ is the Arrhenius frequency factor, $R$ is the ideal gas constant (8.314 J. $mol^{-1}.K^{-1}$) and $T$ is the adsorption temperature (K).

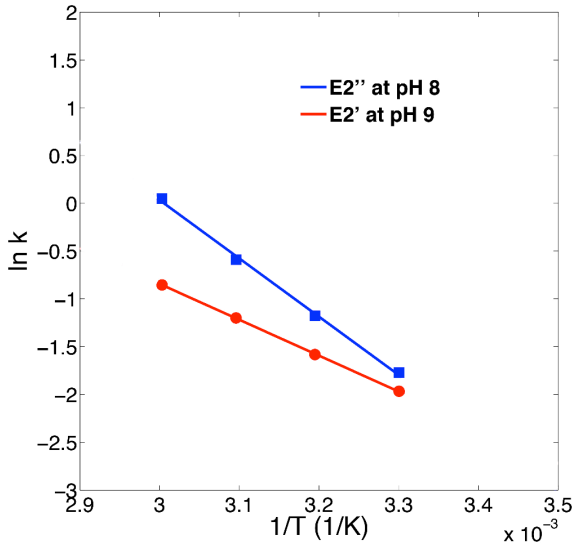


**Figure 3.13.** Plot of ln $k$ vs $1/T$ for E2'' at pH 8 and E2' at pH 9 aerogels. Initial aerogel dose = 100 mg; initial MB concentration = 15 mg/L (46 µM); contact time = 4 h; solution volume = 30 mL.

Plotting ln $k$ vs $1/T$ (figure 3.13) allowed us to calculate the value of $E_a$ which was found to be 49.4 kJ.$mol^{-1}$ for E2" at pH 8, and 32.2 kJ.$mol^{-1}$ for E2' at pH 9. Both

values exist at the interface between physisorption (5 – 40 kJ.mol$^{-1}$) and chemisorption (40 – 800 kJ.mol$^{-1}$) ranges [144] which suggests that both adsorption phenomena do take place, a revelation that is in excellent agreement with what was discussed in previous sections.

**J. Thermodynamic study**

The change in Gibbs free energy $\Delta G°$ of the adsorption can be calculated according to the following equation:

$$\Delta G° = -RT \ln K_C \tag{3.16}$$

where $K_C$ is the equilibrium constant, calculated as the ratio of the concentration of dye on adsorbent at equilibrium ($q_e$) to the remaining concentration of dye at equilibrium ($C_e$). The equilibrium was considered attained after 4 hours.

$$K_C = \frac{q_e}{C_e} \tag{3.17}$$

It is worth mentioning that a slight decrease in the value of $K_C$ was noted with increase in temperature, indicating that the adsorption is thermodynamically stable [145].

On the other hand, $\Delta G°$ can also be calculated from the following equation:

$$\Delta G° = \Delta H° - T\Delta S° \tag{3.18}$$

where $\Delta H°$ is the change in the enthalpy of adsorption and $\Delta S°$ is the change in the entropy. The combination of equations 3.16 and 3.28 leads to the Van't Hoff equation, which can be expressed as follows:

$$\ln K_C = -\frac{\Delta H^o}{R}\left(\frac{1}{T}\right) + \frac{\Delta S^0}{R} \tag{3.19}$$

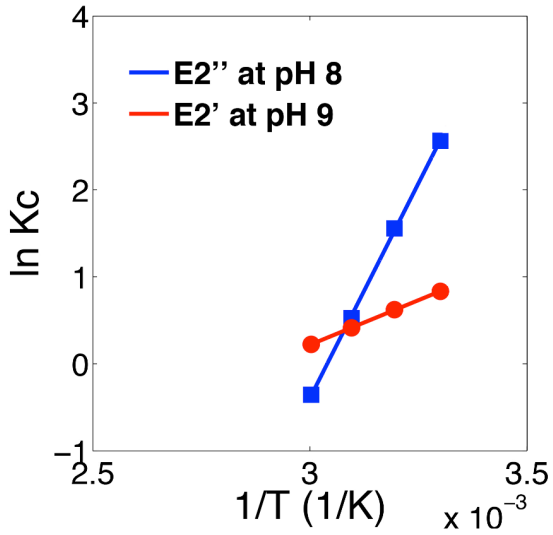


**Figure 3.14.** Plot of ln$K_C$ vs 1/$T$ for E2'' at pH 8 and E2' at pH9 aerogels. Initial aerogel dose = 100 mg; initial MB concentration = 15 mg/L (46 µM); contact time = 4 h; solution volume = 30 mL.

Plotting ln $K_C$ vs 1/$T$ allows the calculation of $\Delta H°$ and $\Delta S°$ from the slope and the intercept respectively of the linear plot (figure 3.14). The results show that enthalpy of adsorption $\Delta H°$ was -86.9 kJ.mol$^{-1}$ and $\Delta S°$ was -264.6 J.mol$^{-1}$.K$^{-1}$ for E2" at pH 8, and -17.6 kJ.mol$^{-1}$ and -51.1 J.mol$^{-1}$.K$^{-1}$ respectively for E2' at pH 9. The standard free energy change $\Delta G°$ was calculated, using Eq. (3.18), to be -6.7 kJ.mol$^{-1}$ for the first and -2.1 kJ.mol$^{-1}$ for the second at 30°C. These value indicate that the adsorption is spontaneous at that temperature, the negative value of $\Delta H°$ is a reflection of an exothermic process and a further indication that adsorption is favored at low temperature, and the negative entropy suggests that the methylene blue molecules were orderly adsorbed on the surface of the silica aerogel. The negative values of $\Delta H°$ and $\Delta S°$ indicate that the adsorption will be spontaneous at lower temperatures [146].

## K. Conclusion

A complete and detailed adsorption study of methylene blue from aqueous solutions onto highly porous phenyl-functionalized silica aerogels was performed where the effect of various parameters was tested, and resulted in suggestions of kinetic and thermodynamic models for the process. Studying various silicon precursors showed that the combination revealing the highest adsorption capacity was TEOS-PhTMS, as the phenyl surface functional group offers a high degree of delocalization, with π-π stacking of the benzene rings on the surface of the gel and the aromatic groups of the methylene blue dye. Varying the solvent in which the gel is synthesized had a notable effect on its adsorption capacity, however no clear trend could be found.

Adsorption studies showed that these surface functionalized silica aerogels are highly efficient methylene blue adsorbents, especially at optimum pH and precursor conditions. Extremely fast adsorption of the dye was noticed within the first 30 minutes of the experiment (more than 70% of the initial dye amount on 100 mg of gel). Particle size has proven to be a crucial factor in the adsorption, as crushing the aerogel particles into a fine powder made the adsorption extremely faster due to the increase in contact surface area between the gel and the dye solution.

The adsorption experimental data fitted with theoretical models met the Sips adsorption isotherm model with up to 49.2 mg of dye adsorbed per gram of adsorbent. The kinetics of the experiments follow a pseudo-second order kinetic model indicating that the adsorption involves both chemisorption and physisorption. The thermodynamic study revealed an exothermic and ordered adsorption process.

# CHAPTER IV

# SELECTIVE ADSORPTION OF XANTHENES AND PAHs ONTO MOLECULARLY-IMPRINTED SILICA SOL-GEL MATERIALS

One application of modified silica aerogels has been thoroughly presented in chapter III. In this chapter another will be investigated: molecular-imprinting. This technique has never been before performed on aerogels to our knowledge. For this reason, even though a detailed strategy was devised for the completion of this project, the unpredictability of it made it difficult to advance at a fast pace. Promising results saw the light nonetheless, and two main fronts were opened: molecular imprinting with caffeine to target theophylline with applications in drug targeting and delivery on the one hand, and molecular imprinting with 2-naphthol to target the specific removal of PAHs.

## A. Experimental description

All adsorption experiments were performed in glass vials placed in a Julabo SW 23 controlled-temperature shaking water bath, operating at 160 rpm and 30°C. In a typical experiment, an initial amount of the adsorbent was dropped in 30 mL of 50 mg/L (0.28mM) theophylline solutions for caffeine-imprinted gels, and 30 mL of 10 μM PAH solutions for 2-naphthol-imprinted gels.

***1. Adsorption of theophylline onto caffeine molecularly-imprinted sol-gel materials.***

The adsorption capacity of caffeine molecularly-imprinted materials was evaluated by following the decrease of the adsorbate concentration over time. 100-µL aliquots were carefully withdrawn from the solution at pre-determined time intervals over 4 h, and then microfiltered to eliminate gel particles if present before analysis on HPLC/UV. HPLC measurements were performed at the two maximum wavelengths of theophylline determined through UV detection: 205.4 and 272.16 nm (figure 4.1).

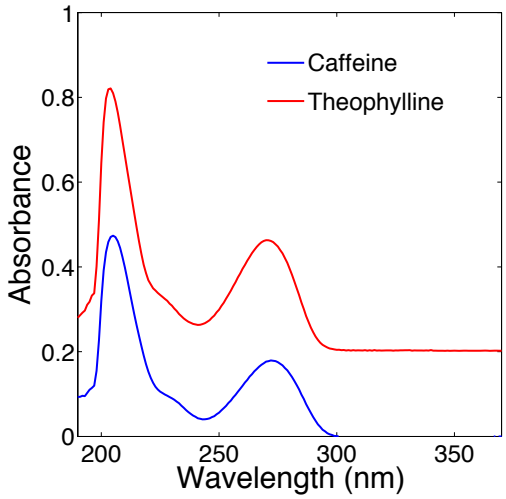


**Figure 4.1.** UV-VIS spectra of caffeine and theophylline in DDW.

Only the peak at 272.16 nm was monitored as it proved to be the more reliable one, with fewer fluctuations than the one at 205.4 nm. The HPLC conditions were as follows: a $C_{18}$ column was used equipped with a guard column, with methanol and a $KH_2PO_4/K_2HPO_4$ phosphate buffer as eluents, with the ratios 25/75%. Phosphate buffer was used instead of regular double distilled or deionized water to maintain the pH at 7.00, as it is a parameter that will affect adsorption results. The eluent flow was 1.00 mL/min, and the injection volume was taken to be 10 µL with needle wash in double

distilled water (DDW). Standards of caffeine and theophylline solutions were run, showing retention times of 11.1 and 7.5 min respectively (figure 4.2). Thus, the cycle time was chosen to be 15 min, well above the retention time of caffeine, to ensure that no amounts of this molecule are released in the system. Upon performance of the experiment, we obtained only 1 peak at a retention time of 7.5 min, indicating that no detectable caffeine is being released, and confirming the complete removal of caffeine from our aerogels. The concentrations were determined by comparing the results to a freshly prepared calibration curve.

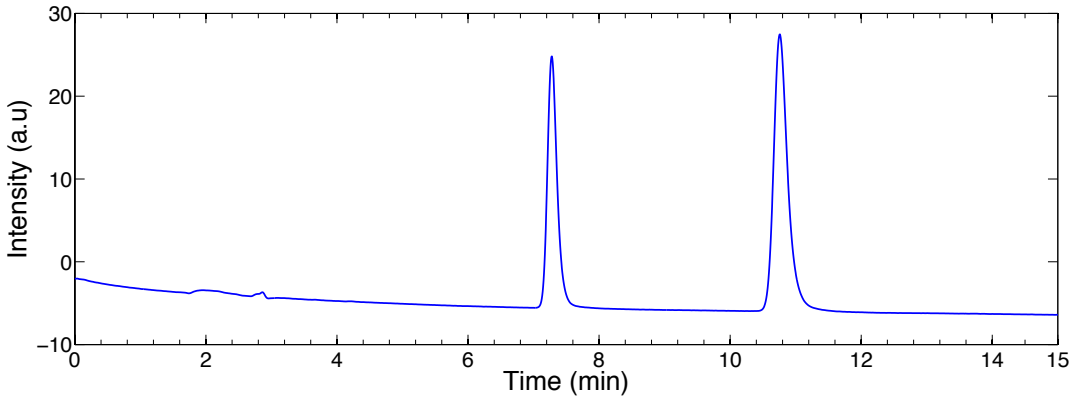


**Figure 4.2.** HPLC chromatograph of an aqueous caffeine/theophylline mixture.

The chemical structures of caffeine and theophylline are shown in figure 4.3. These two molecules were chosen for their structural resemblance, and possible uses in pharmaceutical and medical applications, especially for drug targeting and controlled release applications.

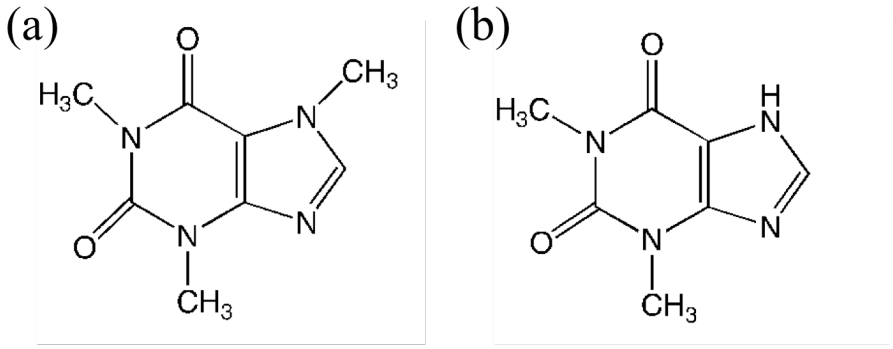


**Figure 4.3.** Molecular structures of (a) caffeine and (b) theophylline.

The parameters studied were varying the alkoxide precursor; TMOS, TMOS-PhTMS, TMOS-VTMS and TMOS-APTES combinations were tried. Also, the impact of caffeine molar ratio on final adsorptive capacity as well as specificity was investigated within the range of 0 (non-imprinted) and 0.15. The water to silica ratio (R) of the gels was monitored as well, noting a difference in behavior with changing R.

***2. Adsorption of PAHs onto 2-naphthol molecularly-imprinted sol-gel materials.***

For the 2-naphthol imprinting experiments, aliquots were carefully withdrawn from the solution with a micropipette at pre-determined time intervals over 4 h, and then analyzed with a Jobin-Yvon Horiba Flurolog-3 fluorometer, with MicroMax 384 micro plate reader and DataMax V2.2 acquisition and analysis software. The results were compiled after analysis of the synchronous fluorescence spectra obtained with an offset of 10 nm (figure 4.4), after determining the excitation and emission spectral data of the PAHs used. Fluorescence peak areas were measured over time and then fitted to a carefully drawn calibration curve to relate them to concentration. Four PAHs were chosen to conduct experiments on: pyrene, anthracene, naphthalene and 2-naphthol

(figure 4.5) . As the miscibility of these PAHs with water is limited, they were dissolved a 10% methanol/DDW binary solvent, which was able to dissolve them completely.

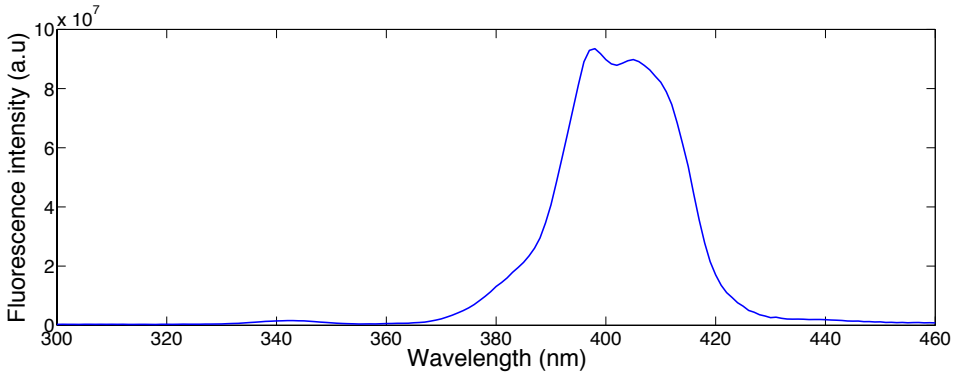


**Figure 4.4.** Synchronous fluorescence spectrum of a mixture of anthracene/2-naphthol; Offset = 10 nm.

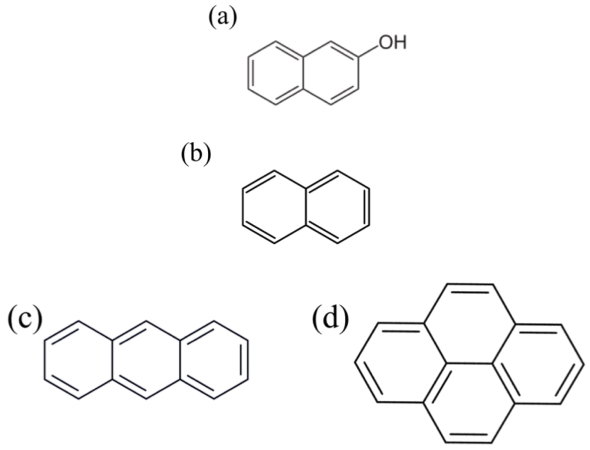


**Figure 4.5.** Chemical structures of (a) 2-naphthol; (b) naphthalene; (c) anthracene and (d) pyrene.

For both types of experiments, the amount of adsorbed material on the silica gels was calculated according to equation 3.1. The alcogels were dropped as a whole in the solution vials, while 100 mg of aerogels was used.

The parameters studied for this part of the work were varying the PAH molecule and the impact of light on adsorption. Competition experiments between different target molecules were performed on both types of imprinted gels to test for selectivity, or their affinity to their respective target molecules.

## B. Caffeine molecularly-imprinted alcogels and aerogels

### *1. Effect of silicon precursor on adsorption of theophylline*

Several silicon precursor combinations were tested for their effect on both final adsorptive capacity on the one hand, and molecular recognition on the other. To that end, TMOS, TMOS-VTMS, TMOS-PhTMS and TMOS-APTES alcogels were synthesized and tested for adsorption of theophylline. In a first attempt, the gels were not imprinted with caffeine, to determine the effect of the precursor alone. The next attempt included imprinting the gels with caffeine. The molar ratio of caffeine with respect to silica was kept constant at 0.15 for the purpose of these experiments. Results show that silicon precursors do possess an important effect on the final adsorptive capacity of alcogels, with the TMOS-PhTMS gel standing out as the one showing the highest adsorption (figure 4.6). For the TMOS and TMOS-APTES alcogel, the OH surface groups make for strong hydrogen bonding between the gel and the theophylline, whereas for the TMOS-VTMS, the vinyl surface groups allow for good pi-delocalization, and very stable bonds with the theophylline molecule. The aromatic rings on the surface of the TMOS-PhTMS functionalized gel offer a much higher degree of delocalization, with $\pi$- $\pi$ stacking between the phenyl groups on the surface of the gel and the aromatic groups of the theophylline molecules, as discussed in previous sections.

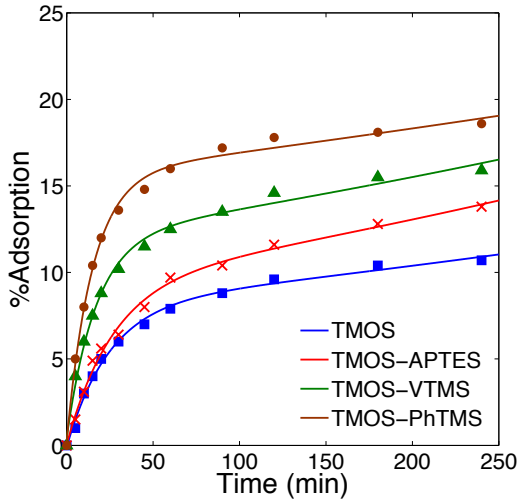


**Figure 4.6.** %Removal of theophylline as a function of time for TMOS, TMOS-APTES, TMOS-VTMS and TMOS-PhTMS non-imprinted alcogels. Initial theophylline concentration = 50 mg/L (0.28 mM); contact time = 4 h; solution volume = 30 mL.

With that being said, the explanation given above does not seem to account for any molecular recognition between the gel and theophylline, as is shown in figure 4.7.

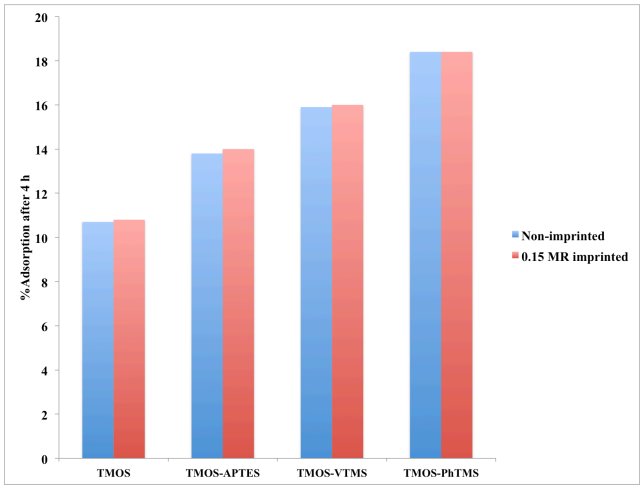


**Figure 4.7.** Comparison of the %Adsorption of theophylline by TMOS, TMOS-APTES, TMOS-VTMS and TMOS-PhTMS non-imprinted and 0.15 MR caffeine imprinted alcogels. Initial theophylline concentration = 50 mg/L (0.28 mM); contact time = 4 h; solution volume = 30 mL.

Aerogels should show better properties and results in adsorption than alcogels because the absence of residual solvent and water in the gel makes adsorption easier. For that reason, subsequent work was performed solely on aerogels. One silica precursor combination was also chosen: TMOS-PhTMS. This gel showed the best adsorptive capacity out of all that were tried; the next step is to try to improve its molecular recognition abilities.

***2. Effect of caffeine molar ratio***

The variation of the molar ratio of caffeine has been studied with the synthesis of TMOS-PhTMS aerogels containing caffeine with molar ratios within the range of 0.05 to 0.15 with respect to silica. Molar ratios above 0.15 were not sudied, because they were above the solubility limit of caffeine in the amounts of DDW and methanol used. A control gel that had no caffeine was synthesized for the sake of comparison, and underwent the same procedural steps as its imprinted analogues, to ensure cohesion of results, and elimination of variables.

Figure 4.8 shows clearly that the molar ratio of caffeine plays a crucial role on the final adsorptive capacity of the gel after 4 hours. The gel with the best adsorptive capacity is the one having a caffeine molar ratio of 0.075. Above that number, the adsorptive capacities of the gels drop back down again. This may be due to an oversaturation of the material in caffeine at high molar ratios during the synthesis process, altering the surface area and porosity of the finished material. Another explanation could be that with high concentrations of caffeine in the gel, aggregation of the template molecules occur, thus no additional selective sites would be created, which would be translated in a reduction of the selective capacity of the material. For these

reasons, all molecularly-imprinted gels synthesized subsequently were prepared at the optimal caffeine molar ratio of 0.075.

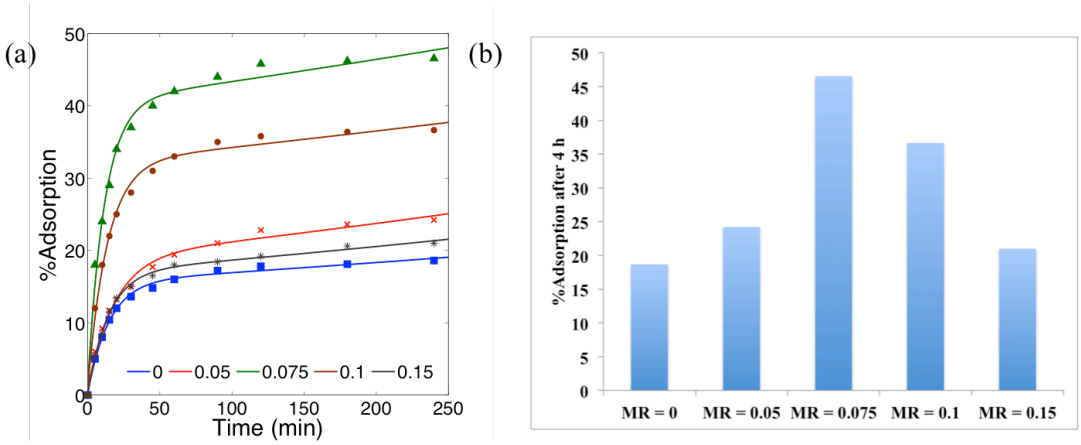


**Figure 4.8.** Comparison of the %Adsorption of theophylline by TMOS-PhTMS non-imprinted and 0.05; 0.075; 0.1 and 0.15 MR caffeine imprinted aerogels as (a) %Adsorption vs time and (b) %Adsorption after 4 h vs caffeine molar ratio. Initial theophylline concentration = 50 mg/L (0.28 mM); initial aerogel dose = 100 mg; contact time = 4 h; solution volume = 30 mL.

3. ***Effect of water to silica ratio***

The reason this parameter was studied was that it possesses an effect in the synthesis of the gel, and ultimately on the structure of the final sol-gel material. In fact, water plays three important roles in the synthesis of gels: it hydrolyzes the reactants, is a product of the condensation reactions and plays the third role of porogen, a role many seem to overlook. All in all, a greater quantity of water will result in bigger pores and a porous material with a looser structure, but at the same time might cause the structure to collapse and reduce the volume of pores in the material [123].

Four aerogels were thus synthesized: TMOS-PhTMS with R = 6 (the water to silica ratio that has been in use through the entirety of this work) and TMOS-PhTMS

with R = 7, both imprinted with caffeine and non-imprinted. Results show that as R increases from 6 to 7, a very notable change in adsorptive capacity after four hours as well as the specificity of the imprinted gels is increased (figure 4.9).

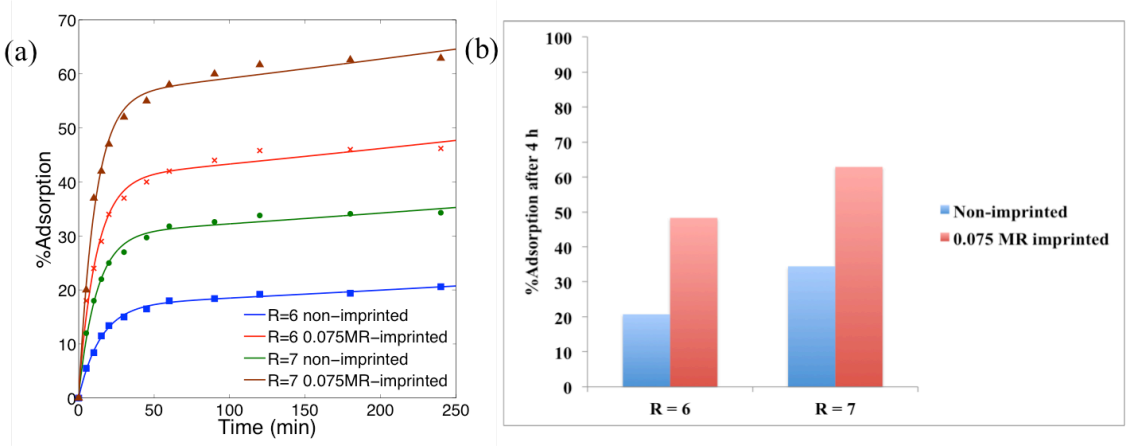


**Figure 4.9.** Comparison of the %Adsorption of theophylline by TMOS-PhTMS non-imprinted and 0.075 MR caffeine imprinted aerogels with water to silica ratio = 6 and 7. (a) %Adsorption vs time and (b) %Adsorption after 4 h vs water to silica molar ratio. Initial theophylline concentration = 50 mg/L (0.28 mM); initial aerogel dose = 100 mg; contact time = 4 h; solution volume = 30 mL.

Caffeine and theophylline have a size of approximately 1 nm [123], so it is intuitive that the material synthesized to adsorb them needs to have pore sizes not smaller than 1 nm, all the more reason for desired mesoporisity. However, as well as high adsorptive capacity, the material needs to have high selectivity for the template molecule over others. And by increasing R, thus making the pores bigger, some selectivity might be lost due to the fact that the gel is enabled to adsorb a much wider array of materials due to its larger pore sizes. A balance between adsorptive capacity and molecular recognition needs to be found with varying the water to silica ratio.

### *4. Selectivity studies*

Competition adsorption experiments were performed, where solutions containing 50 mg/L of both theophylline (0.28 mM) and caffeine (0.26 mM) were prepared, and adsorption experiments with TMOS-PhTMS aerogels with caffeine molar ratio of 0.075 and R ratio of 7, as well as a standard non-imprinted gel as a reference, were conducted and results monitored by HPLC.

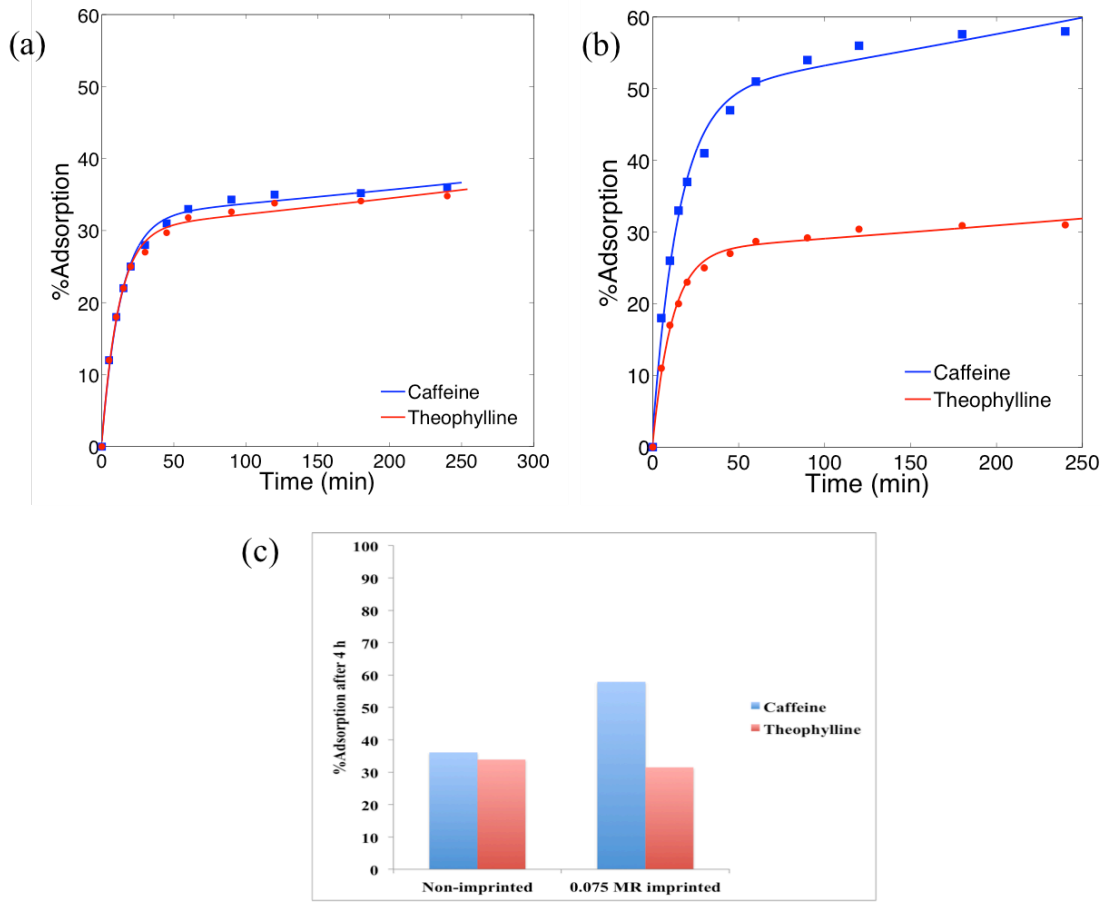


**Figure 4.10.** Comparison of the %Adsorption of caffeine and theophylline by (a) TMOS-PhTMS non-imprinted and (b) TMOS-PhTMS 0.075 MR caffeine imprinted aerogels. (c) Histogram comparing final adsorptive capacities with imprinted and non-imprinted aerogels. Initial caffeine concentration = 50 mg/L (0.26 mM); initial theophylline concentration = 50 mg/L (0.28 mM); initial aerogel dose = 100 mg; contact time = 4 h; solution volume = 30 mL.

Results of these competition experiments show that the synthesized molecularly-imprinted aerogels show a higher affinity for the adsorption of caffeine, with a selectivity (α) of 1.84 calculated by the following equation:

$$\alpha = \frac{\%Ads_{caff}}{\%Ads_{theo}} \tag{4.1}$$

By that formula, a selectivity equal to 1 would mean that there was absolutely no preferential binding of one molecule over another. Results show that the non-imprinted reference gel shows almost no selectivity (α = 1.06) towards any of the two molecules, and adsorbs them almost exactly the same (figure 4.10).

**C. Molecular imprinting with 2-naphthol**

1. ***Adsorption results***

In a typical adsorption experiment, the gels that were used were TMOS-PhTMS 2-naphthol-imprinted aerogels (with a molar ratio of 0.075), as well as a non-imprinted aerogel to serve as reference. The PAH used as adsorbate solution was anthracene in the concentration of 10 μM in a 10% methanol in water solvent. The aliquots were run through a fluorescence spectrometer, where the results were compiled by integrating the synchronous fluorescence peak area between 355 to 466 nm, the peaks attributed to anthracene. Initial results showed little to no difference between imprinted and non-imprinted aerogels (figure 4.11).

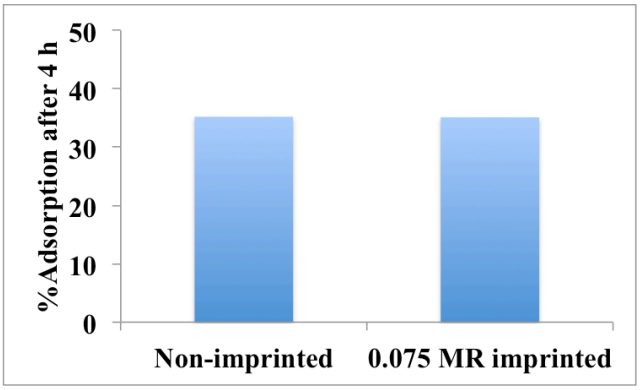


**Figure 4.11.** Comparison of the %Adsorption of anthracene by TMOS-PhTMS non-imprinted and 0.075 MR 2-naphthol imprinted aerogels. Initial anthracene concentration = 10 μM; initial aerogel dose = 100 mg; contact time = 4 h; solution volume = 30 mL.

Upon closer inspection of the results, the peaks attributed to anthracene did not seem to decrease due to the effect of gel adsorption alone, as initial measurements made for determining the initial concentration prior to dropping the gel showed noticeable fluctuations. As there the anthracene solutions contain only the PAH with the solvent, the most plausible explanation for this phenomenon is that light has an effect on the solution. This leads us to believe that a photochemical reaction might be taking place, which will be examined in a subsequent section.

### *2. Effect of light*

A solution containing 10 μM anthracene in 10:90% methanol:DDW was prepared, and fluorescence measurements were performed on aliquots taken over an hour (figure 4.12). The measurements the signal corresponding to anthracene is decreasing over time for the solution exposed to light, while it remains virtually unchanged for the one kept in darkness, indicating that a photochemical reaction is taking place. Accordingly, experiments were subsequently performed in darkness. To

achieve this, the vials and other glassware used for the synthesis were wrapped in aluminum foil before putting in the gel, and kept in darkness for the duration of the experiment, thus making sure that the PAH solutions never got exposed to light.

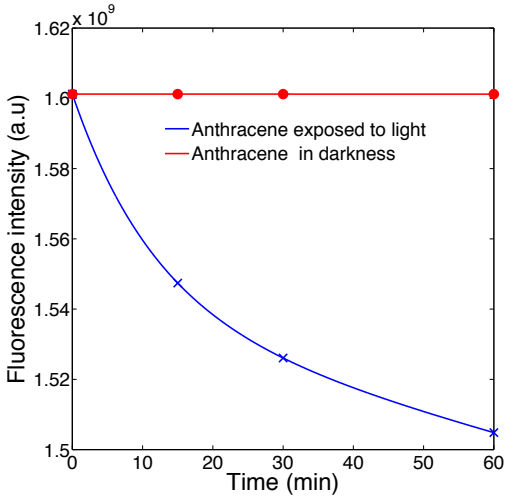


**Figure 4.12.** Fluorescence measurements vs. time of anthracene exposed to light and kept in darkness. Initial anthracene concentration = 10 μM; experiment duration = 60 min.

More promising results came from making this alteration, portrayed in figure 4.13, which shows a slightly better adsorptive capacity than previously, and a very slightly better affinity for anthracene for the imprinted gel. This means that the anthracene molecule is being targeted more efficiently (even if only slightly so) by the 2-naphthol imprinted gels, since the surface of the pores has a structure both morphologically and chemically complementary. For these reasons, the experiments reported in the next section were performed in darkness.

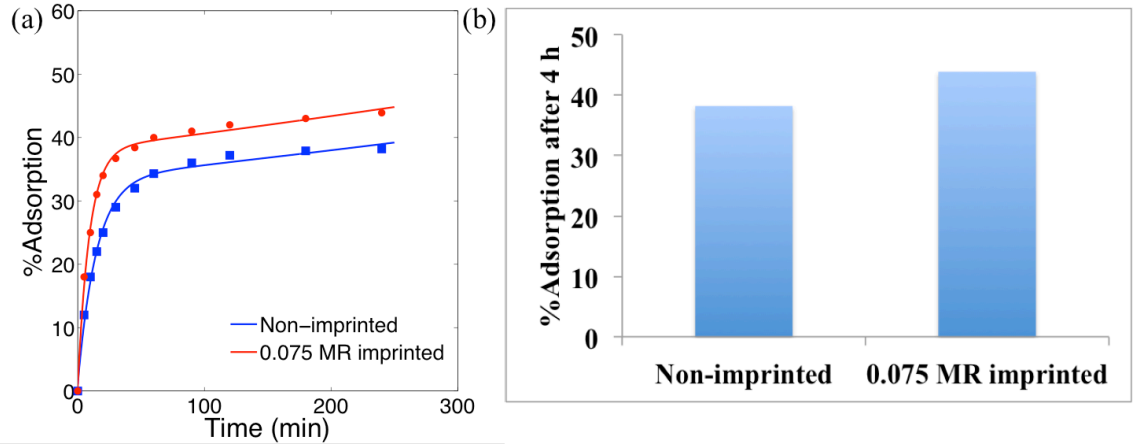


**Figure 4.13.** Comparison of the %Adsorption of anthracene by TMOS-PhTMS non-imprinted and 0.075 MR 2-naphthol imprinted aerogels in dark conditions. (a) %Adsorption vs time; (b) %Adsorption after 4 h vs nature of the aerogel. Initial anthracene concentration = 10 μM; initial aerogel dose = 100 mg; contact time = 4 h; solution volume = 30 mL.

3. ***Effect of PAH***

Four different PAHs were chosen to study their effect on adsorption: anthracene, pyrene, naphthalene and 2-naphthol. Arranged in order of increasing molecular weight: naphthalene, 2-naphthol, anthracene and pyrene. The experimental conditions and the gel nature were kept identical to the ones described previously, but 10 μM solutions of the above-mentioned PAHs in binary solvent were used as target molecules.

As expected, results show that the nature of the PAH has a tremendous effect on adsorption (figure 4.14a) and selectivity (figure 4.14b), with 2-naphthol showing the highest adsorptive capacity and selectivity, followed by naphthalene, anthracene and pyrene due to the resemblance of 2-naphthol and naphthalene, both morphologically and with respect to their size.

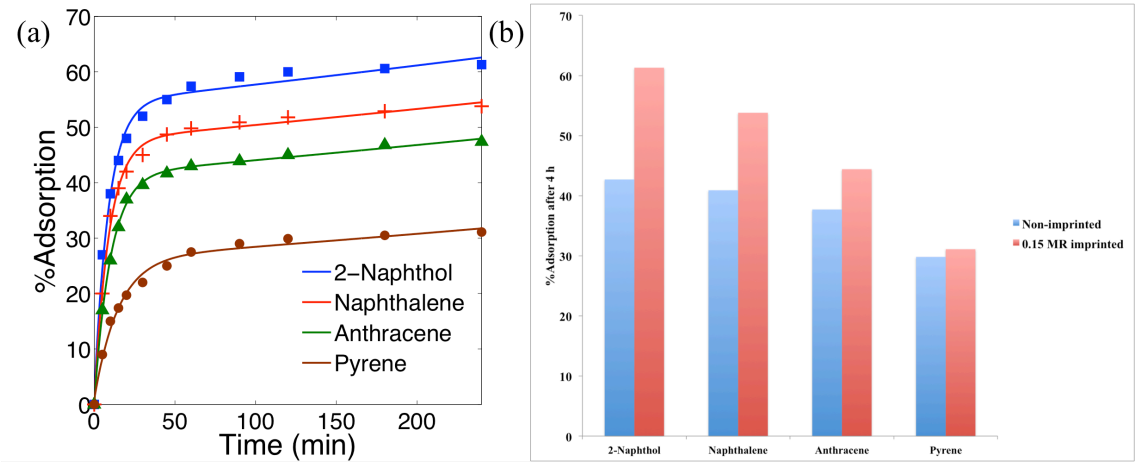


**Figure 4.14.** (a) % Removal of different PAHs vs time by 0.075 MR 2-naphthol imprinted TMOS-PhTMS aerogels in dark conditions. (b) Comparison of %Adsorption of different PAHs by non-imprinted and 0.075 MR 2-naphthol imprinted TMOS-PhTMS aerogels in dark conditions. Initial PAH concentration = 10 µM; initial aerogel dose = 100 mg; contact time = 4 h; solution volume = 30 mL.

A correlation can thus be drawn between the adsorptive capacity of the 2-naphthol imprinted silica aerogels and the structure of the target molecule, wherein the closer the resemblance the better the adsorptive capacity and selectivity. This means that the imprinting is efficient, but the bigger and bulkier the adsorbate molecule, the less the effect of imprinting is appearing.

### *4. Selectivity studies*

Competition experiments were undergone, where 2-naphthol was chosen as reference molecule, since it was the one showing the best adsorption results and selectivity. Two other test molecules were tried in two different experiments: naphthalene, and anthracene. In the first experiment, the aerogels were dropped in an equimolar mixture of 10 µM 2-napthol/anthracene, and in the second, they were dropped in an equimolar mixture of 10 µM 2-napthol/naphthalene (figure 4.15).

As expected, when compared to naphthalene, the 2-naphthol imprinted aerogels showed slightly better selectivity towards 2-naphthol (α = 1.09 ), whereas the effect became much more pronounced when compared to the bulkier anthracene (α = 1.21). However, the non-imprinted aerogel showed relatively no selectivity whatsoever: α = 1.00 when 2-naphthol was compared with naphthalene, and α = 1.02 when 2-naphthol was compared with anthracene. These values show that the imprinted materials are more selective towards their target molecules than non-imprinted materials.

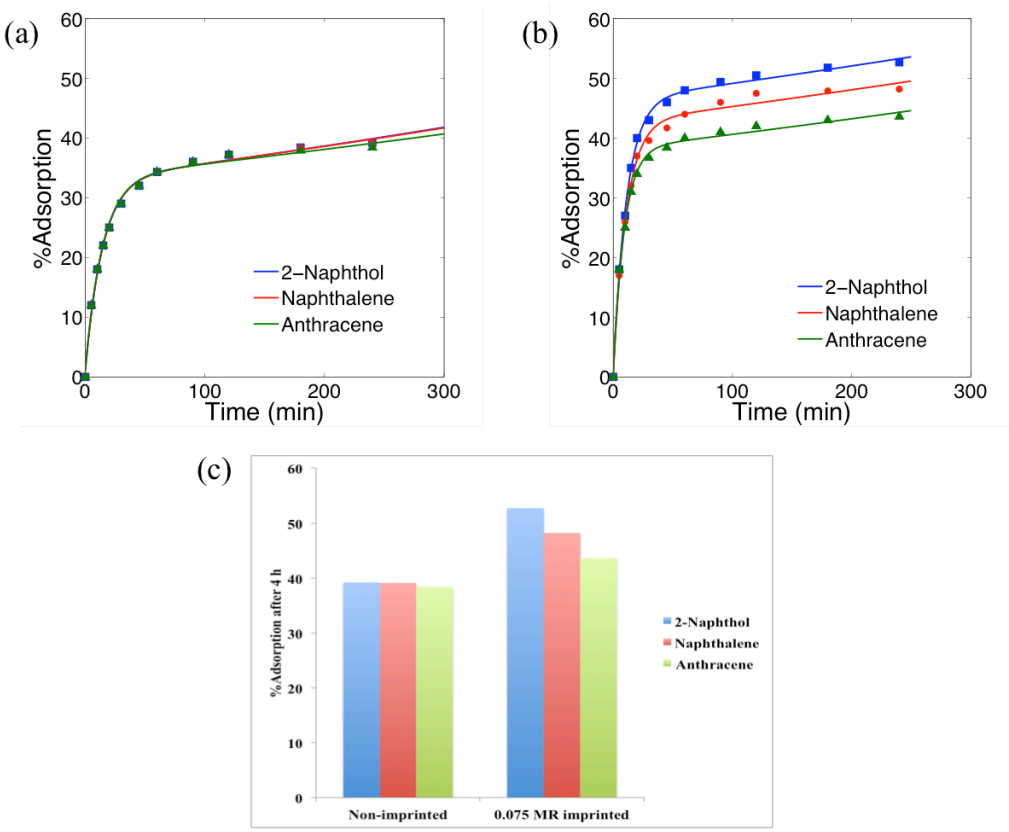


**Figure 4.15.** Comparison of the %Adsorption of 2-naphthol, naphthalene and anthracene by (a) TMOS-PhTMS non-imprinted and (b) TMOS-PhTMS 0.075 MR 2-naphthol imprinted aerogels in dark conditions. (c) Histogram comparing final adsorptive capacities with imprinted and non-imprinted aerogels. Initial 2-naphthol concentration = 10 µM; initial naphthalene concentration = 10 µM; initial anthracene concentration = 10 µM; initial aerogel dose = 100 mg; contact time = 4 h; solution volume = 30 mL.

## D. Conclusion

As a conclusion to this part of the work, molecular imprinting of silica aerogels with caffeine and 2-naphthol was successful. Varying the molar ratio of the template, the silicon precursor nature, as well as the water to silica ratio had a pronounced effect on both adsorptive capacity and selectivity, with 0.075 and phenyl-functionalized TMOS being the best molar ratio of template with respect to silica and precursor combination respectively, and R = 7 showing better adsorption profiles than R = 6. Varying different parameters such as adsorbate nature and exposure to light had an impact on the adsorption of PAHs by 2-naphthol molecularly-imprinted aerogels.

Work still needs to be done on fine-tuning the obtained results to find materials that could compete with other MIPs now available, but nonetheless results indicate that this could be achieved in the near future.

# CHAPTER V

# SUMMARY AND CONCLUSIONS

## A. **Summary and conclusions**

A complete and detailed overview of the synthesis of surface-functionalized and molecularly-imprinted silica alcogels and aerogels was presented, as well as full characterization of the obtained solid-state materials by FTIR spectroscopy and SEM. These techniques revealed surface functionalization to be a success, adding surface functional groups without altering to the core structure of the gel. Furthermore, in the cases where molecular imprinting was involved, results showed that the template material was completely removed in the final structure of the gel, with no alterations to its core structure.

A complete and detailed adsorption study of methylene blue from aqueous solutions onto highly porous phenyl-functionalized silica aerogels was performed where the effect of various parameters was tested, and resulted in suggestions of kinetic and thermodynamic models for the process. A study of various silicon precursors showed that surface functionalization has a crucial effect on adsorptive capacity, which increases with increasing degree of delocalization at the surface of the gel. Varying the solvent in which the gel is synthesized had a notable effect on its adsorption capacity, however no clear trend could be found.

Adsorption studies showed that these surface functionalized silica aerogels are highly efficient methylene blue adsorbents, in which the best silicon precursor/solvent

combination was determined and subsequently thoroughly investigated. Particle size has proven to be a crucial factor in the adsorption, as crushing the aerogel particles into a fine powder made the adsorption extremely faster due to the increase in contact surface area between the gel and the dye solution.

The adsorption experimental data fitted with theoretical models met the Sips adsorption isotherm model and the kinetics of the experiments showed that they follow a pseudo-second order kinetic model indicating that the adsorption involves both chemisorption and physisorption. The thermodynamic study revealed an exothermic and ordered adsorption process. In conclusion, this part of the study showed the phenyl-functionalized silica aerogel to be a highly efficient adsorbing material for methylene blue, highly customizable, fine-tunable and economically very attractive.

An adsorption study of the specific adsorption of theophylline and PAHs from aqueous solutions onto caffeine and 2-naphthol molecularly-imprinted silica aerogels respectively, where various parameters were tested and resulted in a better understanding of the specific adsorption process. Slightly modifying the $CO_2$ supercritical drying method to include two 24 h solvent exchange steps instead of just the one with acetone proved to be extremely effective and resulted in complete removal of the template molecule; an important achievement since it drastically reduced production times with no risk to the final solid material, and more importantly since it resulted in the first ever synthesized molecularly-imprinted silica aerogels (to our knowledge).

A study of various silicon precursors reaffirmed their effect on adsorptive capacity and selectivity, along with varying the molar ratio of the template was found to give optimal results. The water to silica ratio was also varied with higher R showing

better results both in adsorptive capacity and selectivity, due to a slight increase in the size of the pores because of the higher amount of water present during hydrolysis.

The PAH solutions were found to undergo a photochemical reaction with visible light, which hindered adsorption measurements. As a result, all adsorption measurements were conducted in darkness for the case of 2-naphthol imprinting for the targeting of PAHs. These target molecules were found to affect the adsorption with anthracene, pyrene, naphthalene and 2-naphthol tested as adsorbates. Adsorption of 2-naphthol proved to be the most effective and the most selective, followed by naphthalene. This is due to the structural resemblance naphthalene bears with 2-naphthol, in contrast with the bulkier pyrene and anthracene.

Equimolar mixtures of two template molecules were prepared, and competition experiments were performed, revealing that the imprinted gel has a much higher adsorptive capacity and selectivity towards its own template molecule. All in all, this project is still in its early phases of development, but encouraging results were obtained, indicating there are still loads to explore.

**B. Future work**

Surface functionalized aerogels for the adsorption of methylene blue was studied in great detail, but work still remains to be done in testing for the reusability of the material by performing successive adsorption/desorption experiments for the same gel, and the variation of other variables such as the PhTMS to TEOS molar ratio. This will help pave the way to a more industrial application of these materials in wastewater treatment and water management for industrial plants.

In the work on molecularly-imprinted silica aerogels, a lot still remains to be done. Since the synthesis of this material has proven to be possible, work should now be focused on fine-tuning its properties in order to make it a contender in specific adsorption, and later on in pharmaceutical applications such as drug targeting and controlled release. Environmental applications could also be envisaged for this material such as the targeted removal of the highly toxic PAHs from wastewater, while leaving other chemicals that are beneficial to the water's ecosystem intact.

On the one hand, the effect of synthesis solvent should be explored since different solvents resulted in different adsorptive capacities for the case of surface functionalized silica aerogels. Moreover, a crucial pH study should be conducted as it is one of the parameters having the most effect on adsorption. Moreover, a full study on the effect of water to silica ratio should be performed, covering a much broader range of R, to investigate the relation between selectivity and adsorptive capacity and find the optimum R.

The effect of particle size, dose and initial adsorbate concentrations should be explored in an attempt to fine-tune the adsorption. The effect of temperature should also be studied to elucidate the adsorption kinetic and thermodynamic models, which would help a great deal in better understanding this phenomenon, and the effect of imprinting in particular. Finally, adding porogens such as lactic acid to the synthesis, as well as investigating the concentration of the base during hydrolysis and condensation should be investigated, as studies show that they play a role in the adsorptive capacity and selectivity of molecularly-imprinted polymers [123, 147].

# REFERENCES


1. Patel, R.P., N.S. Purohit, and A.M. Suthar, *An overview of silica aerogels.* Int. J. Chem. Tech. Res, 2009. **1**: p. 1052-1057.

2. Gurav, J.L., et al., *Silica Aerogel: Synthesis and Applications.* Journal of Nanomaterials, 2010. **2010**.

3. Brinker, C. and G. Scherer, *Sol-Gel Science: The Physics and Chemistry of Sol-Gel Processing*. 1990: Academic. No pp. given.

4. Hench, L.L. and J.K. West, *The sol-gel process.* Chemical Reviews, 1990. **90**(1): p. 33-72.

5. Ébelmen, J.J., *Recueil des travaux scientifiques de m. Ébelmen, revu et corrigé par m. Salvétat, précédé d'une notice sur m. Ébelmen par E. Chevreul*. 1855.

6. Roy, R., *Aids in Hydrothermal Experimentation: II, Methods of Making Mixtures for Both "Dry" and "Wet" Phase Equilibrium Studies.* Journal of the American Ceramic Society, 1956. **39**(4): p. 145-146.

7. Roy, R., *Gel Route to Homogeneous Glass Preparation.* Journal of the American Ceramic Society, 1969. **52**(6): p. 344-344.

8. McCarthy, G.J., R. Roy, and J.M. McKay, *Preliminary Study of Low-Temperature "Glass" Fabrication from Noncrystalline Silicas.* Journal of the American Ceramic Society, 1971. **54**(12): p. 637-638.

9. Iler, R.K., *The Colloid Chemistry of Silica and Silicates*. 1955: Cornell Univ. Press. 324 pp.

10. Stöber, W., A. Fink, and E. Bohn, *Controlled growth of monodisperse silica spheres in the micron size range.* Journal of colloid and interface science, 1968. **26**(1): p. 62-69.

11. Overbeek, J.T.G., *Monodisperse colloidal systems, fascinating and useful.* Advances in Colloid and Interface Science, 1982. **15**(3): p. 251-277.

12. Sugimoto, T., *Preparation of monodispersed colloidal particles.* Advances in Colloid and Interface Science, 1987. **28**: p. 65-108.

13. Xu, Y., G. Huang, and Y. He, *Sol-gel preparation of* $Ba_{6-3x}Sm_{8+2x}Ti_{18}O_{54}$ *microwave dielectric ceramics.* Ceramics international, 2005. **31**(1): p. 21-25.

14. Escribano, P., et al., *Low-temperature synthesis of $SrAl_2O_4$ by a modified sol–gel route: XRD and Raman characterization.* Journal of Solid State Chemistry, 2005. **178**(6): p. 1978-1987.

15. Brinker, C.J., *Hydrolysis and condensation of silicates: effects on structure.* Journal of Non-Crystalline Solids, 1988. **100**(1): p. 31-50.

16. Soleimani Dorcheh, A. and M.H. Abbasi, *Silica aerogel; synthesis, properties and characterization.* Journal of Materials Processing Technology, 2008. **199**(1–3): p. 10-26.

17. Livage, J., M. Henry, and C. Sanchez, *Sol-gel chemistry of transition metal oxides.* Progress in Solid State Chemistry, 1988. **18**(4): p. 259-341.

18. Ishizuka, N., et al., *Performance of a monolithic silica column in a capillary under pressure-driven and electrodriven conditions.* Analytical chemistry, 2000. **72**(6): p. 1275-1280.

19. Ishizuka, N., et al., *Designing monolithic double-pore silica for high-speed liquid chromatography.* Journal of Chromatography A, 1998. **797**(1): p. 133-137.

20. Minakuchi, H., et al., *Octadecylsilylated porous silica rods as separation media for reversed-phase liquid chromatography.* Analytical chemistry, 1996. **68**(19): p. 3498-3501.

21. Minakuchi, H., et al., *Effect of skeleton size on the performance of octadecylsilylated continuous porous silica columns in reversed-phase liquid chromatography.* Journal of Chromatography A, 1997. **762**(1): p. 135-146.

22. Wagh, P.B., et al., *Comparison of some physical properties of silica aerogel monoliths synthesized by different precursors.* Materials chemistry and physics, 1999. **57**(3): p. 214-218.

23. Colón, L.A., Y. Guo, and A. Fermier, *Peer Reviewed: Capillary Electrochromatography.* Analytical Chemistry, 1997. **69**(15): p. 461A-467A.

24. Einarsrud, M.A., et al., *Strengthening of silica gels and aerogels by washing and aging processes.* Journal of non-crystalline solids, 2001. **285**(1): p. 1-7.

25. Deng, Z., et al., *Physical properties of silica aerogels prepared with polyethoxydisiloxanes.* Journal of Sol-Gel Science and Technology, 2000. **19**(1-3): p. 677-680.

26. Zhang, X. and S. Huang, *Single step on-column frit making for capillary high-performance liquid chromatography using sol–gel technology.* Journal of Chromatography A, 2001. **910**(1): p. 13-18.

27. Dai, S., et al., *Preparation of silica aerogel using ionic liquids as solvents.* Chem. Commun., 2000(3): p. 243-244.

28. Dieudonné, P., et al., *Transformation of nanostructure of silica gels during drying.* Journal of non-crystalline solids, 2000. **262**(1): p. 155-161.

29. Wu, G., et al., *Properties of sol–gel derived scratch-resistant nano-porous silica films by a mixed atmosphere treatment.* Journal of non-crystalline solids, 2000. **275**(3): p. 169-174.

30. Mezza, P., J. Phalippou, and R. Sempere, *Sol–gel derived porous silica films.* Journal of non-crystalline solids, 1999. **243**(1): p. 75-79.

31. Venkateswara Rao, A., et al., *Synthesis of flexible silica aerogels using methyltrimethoxysilane (MTMS) precursor.* Journal of Colloid and Interface Science, 2006. **300**(1): p. 279-285.

32. Venkateswara Rao, A. and D. Haranath, *Effect of methyltrimethoxysilane as a synthesis component on the hydrophobicity and some physical properties of silica aerogels.* Microporous and Mesoporous Materials, 1999. **30**(2–3): p. 267-273.

33. Zhou, B., et al., *Hydrophobic silica aerogels derived from polyethoxydisiloxane and perfluoroalkylsilane.* Materials Science and Engineering: C, 2007. **27**(5–8): p. 1291-1294.

34. Moner-Girona, M., et al., *Sol-Gel Route to Direct Formation of Silica Aerogel Microparticles Using Supercritical Solvents.* Journal of Sol-Gel Science and Technology, 2003. **26**(1-3): p. 645-649.

35. Kirkbir, F., et al., *Drying and sintering of sol-gel derived large $SiO_2$ monoliths.* Journal of Sol-Gel Science and Technology, 1996. **6**(3): p. 203-217.

36. Judeinstein, P., et al., *Investigation of Ion-Conducting Ormolytes: Structure-Property Relationships.* Chemistry of Materials, 1994. **6**(2): p. 127-134.

37. Gurav, J.L., D.Y. Nadargi, and A.V. Rao, *Effect of mixed Catalysts system on TEOS-based silica aerogels dried at ambient pressure.* Applied Surface Science, 2008. **255**(5): p. 3019-3027.

38. Rao, A.P., G.M. Pajonk, and A.V. Rao, *Effect of preparation conditions on the physical and hydrophobic properties of two step processed ambient pressure dried silica aerogels.* Journal of Materials Science, 2005. **40**(13): p. 3481-3489.

39. Hafidi Alaoui, A., et al., *Room Temperature Densification of Aerogel by Isostatic Compression.* Journal of Sol-Gel Science and Technology, 1998. **13**(1-3): p. 365-369.

40. Pope, E.J.A. and J.D. Mackenzie, *Sol-gel processing of silica: II. The role of the catalyst.* Journal of Non-Crystalline Solids, 1986. **87**(1): p. 185-198.

41. Murata, H., et al., *Drying and sintering of bulk silica gels.* Journal of Sol-Gel Science and Technology, 1997. **8**(1-3): p. 397-402.

42. Bryans, T.R., V.L. Brawner, and E.L. Quitevis, *Microstructure and porosity of silica xerogel monoliths prepared by the fast sol-gel method.* Journal of sol-gel science and technology, 2000. **17**(3): p. 211-217.

43. Vollet, D.R., D.A. Donatti, and A. Ibanez Ruiz, *A SAXS study of kinetics of aggregation of TEOS-derived sonogels at different temperatures.* Journal of non-crystalline solids, 2001. **288**(1): p. 81-87.

44. Karmakar, B., G. De, and D. Ganguli, *Dense silica microspheres from organic and inorganic acid hydrolysis of TEOS.* Journal of non-crystalline solids, 2000. **272**(2): p. 119-126.

45. Hench, L.L. and G. Orcel, *Physical-chemical and biochemical factors in silica sol-gels.* Journal of Non-Crystalline Solids, 1986. **82**(1): p. 1-10.

46. Hench, L.L., G. Orcel, and J.L. Nogues. *The Role of Chemical Additives in Sol-Gel Processing*. in *MRS Proceedings*. 1986. Cambridge Univ Press.

47. Orcel, G., et al., *Effect of formamide additive on the chemistry of silica sol-gels II. Gel structure.* Journal of non-crystalline solids, 1988. **105**(3): p. 223-231.

48. Klemperer, W.G., et al. *Structural characterization of polysilicate intermediates formed during sol-gel polymerization*. in *Mater. Res. Soc. Symp. Proc*. 1988. Cambridge Univ Press.

49. Klemperer, W.G. and S.D. Ramamurthi. *Molecular growth pathways in silica sol-gel polymerization*. in *CJ Brinker, DE Clark, DR Ulrich, Better Ceramics Through Chemistry III, Mater. Res. Soc. Symp. Proc. 121, Pittsburgh, PA*. 1988. Cambridge Univ Press.

50. Aelion, R., A. Loebel, and F. Eirich, *Hydrolysis of Ethyl Silicate*.* Journal of the American Chemical Society, 1950. **72**(12): p. 5705-5712.

51. Artaki, I., et al., *29Si NMR study of the initial stage of the sol-gel process under high pressure.* Journal of Non-Crystalline Solids, 1985. **72**(2–3): p. 391-402.

52. Artaki, I., S. Sinha, and J. Jonas, *Pressure effect on the polymerization kinetics of sol-gel process.* Materials Letters, 1984. **2**(5, Part B): p. 448-450.

53. Artaki, I., T. Zerda, and J. Jonas, *Solvent effects on hydrolysis stage of the sol-gel process.* Materials Letters, 1985. **3**(12): p. 493-496.

54. Nakanishi, K., et al., *Structure Design of Double-Pore Silica and Its Application to HPLC.* Journal of Sol-Gel Science and Technology, 1998. **13**(1-3): p. 163-169.

55. Martin, J., et al., *Mechanical and acoustical properties as a function of PEG concentration in macroporous silica gels.* Journal of Non-Crystalline Solids, 2001. **285**(1–3): p. 222-229.

56. Hæreid, S., E. Nilsen, and M.-A. Einarsrud, *Subcritical drying of silica gels.* Journal of Porous Materials, 1996. **2**(4): p. 315-324.

57. Strøm, R.A., et al., *Strengthening and aging of wet silica gels for up-scaling of aerogel preparation.* Journal of sol-gel science and technology, 2007. **41**(3): p. 291-298.

58. Scherer, G.W., et al., *Shrinkage of silica gels aged in TEOS.* Journal of non-crystalline solids, 1996. **202**(1): p. 42-52.

59. Scherer, G.W. and D.M. Smith, *Cavitation during drying of a gel.* Journal of non-crystalline solids, 1995. **189**(3): p. 197-211.

60. Gross, J., P.R. Coronado, and L.W. Hrubesh, *Elastic properties of silica aerogels from a new rapid supercritical extraction process.* Journal of non-crystalline solids, 1998. **225**: p. 282-286.

61. Poco, J.F., et al. *A rapid supercritical extraction process for the production of silica aerogels*. in *MRS Proceedings*. 1996. Cambridge Univ Press.

62. Scherer, G.W., et al., *Optimization of the rapid supercritical extraction process for aerogels.* Journal of Non-crystalline solids, 2002. **311**(3): p. 259-272.

63. Gauthier, B.M., et al., *A fast supercritical extraction technique for aerogel fabrication.* Journal of non-crystalline solids, 2004. **350**: p. 238-243.

64. Van Bommel, M.J. and A.B. De Haan, *Drying of silica aerogel with supercritical carbon dioxide.* Journal of non-crystalline solids, 1995. **186**: p. 78-82.

65. Ehrburger-Dolle, F., et al., *Relations between the texture of silica aerogels and their preparation.* Journal of non-crystalline solids, 1995. **186**: p. 9-17.

66. Yoda, S. and S. Ohshima, *Supercritical drying media modification for silica aerogel preparation.* Journal of non-crystalline solids, 1999. **248**(2): p. 224-234.

67. Tewari, P.H., A.J. Hunt, and K.D. Lofftus, *Ambient-temperature supercritical drying of transparent silica aerogels.* Materials Letters, 1985. **3**(9): p. 363-367.

68. Tajiri, K. and K. Igarashi, *The effect of the preparation conditions on the optical properties of transparent silica aerogels.* Solar energy materials and solar cells, 1998. **54**(1): p. 189-195.

69. Land, V.D., T.M. Harris, and D.C. Teeters, *Processing of low-density silica gel by critical point drying or ambient pressure drying.* Journal of non-crystalline solids, 2001. **283**(1): p. 11-17.

70. Dimitriev, Y., Y. Ivanova, and R. Iordanova, *History of sol-gel science and technology.* Journal of the University of Chemical technology and Metallurgy, 2008. **43**(2): p. 181-192.

71. Kickelbick, G., *Hybrid inorganic–organic mesoporous materials.* Angewandte Chemie International Edition, 2004. **43**(24): p. 3102-3104.

72. de Aa. Soler-Illia, G.J., et al., *Chemical strategies to design textured materials: from microporous and mesoporous oxides to nanonetworks and hierarchical structures.* Chemical Reviews, 2002. **102**(11): p. 4093-4138.

73. Wen, J. and G.L. Wilkes, *Organic/inorganic hybrid network materials by the sol-gel approach.* Chemistry of Materials, 1996. **8**(8): p. 1667-1681.

74. Sanchez, C., F. Ribot, and B. Lebeau, *Molecular design of hybrid organic-inorganic nanocomposites synthesized via sol-gel chemistry.* Journal of Materials Chemistry, 1999. **9**(1): p. 35-44.

75. Collinson, M.M., *Recent trends in analytical applications of organically modified silicate materials.* TrAC Trends in Analytical Chemistry, 2002. **21**(1): p. 31-39.

76. Lev, O., et al., *Organically modified sol-gel sensors.* Analytical Chemistry, 1995. **67**(1): p. 22A-30A.

77. Livage, J., et al. *Enzymes and Cells Confined in Silica Nanopores*. in *Materials research society symposium proceedings*. 2001. Cambridge Univ Press.

78. Walcarius, A., et al., *Exciting new directions in the intersection of functionalized sol–gel materials with electrochemistry.* Journal of Materials Chemistry, 2005. **15**(35-36): p. 3663-3689.

79. Mann, S., et al., *Sol-gel synthesis of organized matter.* Chemistry of materials, 1997. **9**(11): p. 2300-2310.

80. Asefa, T., et al., *Recent developments in the synthesis and chemistry of periodic mesoporous organosilicas.* Studies in Surface Science and Catalysis, 2002. **141**: p. 1-26.

81. Sayari, A. and S. Hamoudi, *Periodic mesoporous silica-based organic-inorganic nanocomposite materials.* Chemistry of Materials, 2001. **13**(10): p. 3151-3168.

82. Dave, B.C., et al., *Sol-gel encapsulation methods for biosensors.* Analytical Chemistry, 1994. **66**(22): p. 1120A-1127A.

83. Avnir, D., et al., *Enzymes and other proteins entrapped in sol-gel materials.* Chemistry of Materials, 1994. **6**(10): p. 1605-1614.

84. Avnir, D., *Organic chemistry within ceramic matrixes: doped sol-gel materials.* Accounts of chemical research, 1995. **28**(8): p. 328-334.

85. Gupta, G.S., et al., *China clay as an adsorbent for dye house wastewaters.* Environmental Technology, 1992. **13**(10): p. 925-936.

86. Tünay, O., et al., *Use and minimization of water in leather tanning processes.* Water science and technology, 1999. **40**(1): p. 237-244.

87. Ivanov, K., et al., *Possibilities of using zeolite as filler and carrier for dyestuffs in paper.* Papier, 1996. **50**(7-8): p. 456-&.

88. Bhat, R.V. and P. Mathur, *Changing scenario of food colours in India.* Current Science, 1998. **74**(3): p. 198-202.

89. Cook, S.M.F. and D.R. Linden, *Use of rhodamine WT to facilitate dilution and analysis of atrazine samples in short-term transport studies.* Journal of environmental quality, 1997. **26**(5): p. 1438-1440.

90. Wagner, R.W. and J.S. Lindsey, *Boron-dipyrromethene dyes for incorporation in synthetic multi-pigment light-harvesting arrays.(vol 68, pg 1373, 1996).* Pure and applied chemistry, 1998. **70**(8): p. AR1-AR1.

91. Wróbel, D., A. Boguta, and R.M. Ion, *Mixtures of synthetic organic dyes in a photoelectrochemical cell.* Journal of Photochemistry and Photobiology A: Chemistry, 2001. **138**(1): p. 7-22.

92. Scarpi, C., et al., *High-performance liquid chromatography determination of direct and temporary dyes in natural hair colourings.* Journal of Chromatography A, 1998. **796**(2): p. 319-325.

93. Forgacs, E., T. Cserháti, and G. Oros, *Removal of synthetic dyes from wastewaters: a review.* Environment International, 2004. **30**(7): p. 953-971.

94. Abramian, L. and H. El-Rassy, *Adsorption kinetics and thermodynamics of azo-dye Orange II onto highly porous titania aerogel.* Chemical Engineering Journal, 2009. **150**(2–3): p. 403-410.

95. Rafatullah, M., et al., *Adsorption of methylene blue on low-cost adsorbents: A review.* Journal of Hazardous Materials, 2010. **177**(1–3): p. 70-80.

96. Gaikwad, R.W. and S.A. Misal, *Sorption studies of methylene blue on silica gel.* J. Indian Water Works Assoc., 2012. **44**(Copyright (C) 2013 American Chemical Society (ACS). All Rights Reserved.): p. 4-8.

97. Lachheb, H., et al., *Photocatalytic degradation of various types of dyes (Alizarin S, Crocein Orange G, Methyl Red, Congo Red, Methylene Blue) in water by UV-irradiated titania.* Applied Catalysis B: Environmental, 2002. **39**(1): p. 75-90.

98. Kannan, C., T. Sundaram, and T. Palvannan, *Environmentally stable adsorbent of tetrahedral silica and non-tetrahedral alumina for removal and recovery of malachite green dye from aqueous solution.* J. Hazard. Mater., 2008. **157**(Copyright (C) 2013 American Chemical Society (ACS). All Rights Reserved.): p. 137-145.

99. Chen, M., Y. Chen, and G. Diao, *Adsorption Kinetics and Thermodynamics of Methylene Blue onto p-tert-Butyl-calix[4,6,8]arene-Bonded Silica Gel.* Journal of Chemical & Engineering Data, 2010. **55**(11): p. 5109-5116.

100. Pavan, F.A., et al., *Removal of Congo red from aqueous solution by anilinepropylsilica xerogel.* Dyes and Pigments, 2008. **76**(1): p. 64-69.

101. Hirashima, H., H. Imai, and Y. Fukui, *Structure of Hybrid Silica Gels Incorporated with Hydrophobic Dye Molecules.* J. Sol-Gel Sci. Technol., 2003. **26**(Copyright (C) 2013 American Chemical Society (ACS). All Rights Reserved.): p. 383-388.

102. Ghosh, D. and K.G. Bhattacharyya, *Adsorption of methylene blue on kaolinite.* Applied Clay Science, 2002. **20**(6): p. 295-300.

103. Hameed, B.H., A.T.M. Din, and A.L. Ahmad, *Adsorption of methylene blue onto bamboo-based activated carbon: Kinetics and equilibrium studies.* Journal of Hazardous Materials, 2007. **141**(3): p. 819-825.

104. Feng, Y., et al., *Methylene blue adsorption onto swede rape straw (Brassica napus L.) modified by tartaric acid: Equilibrium, kinetic and adsorption mechanisms.* Bioresource Technology, 2012. **125**(0): p. 138-144.

105. Sarioglu, M. and U. Atay, *Removal of methylene blue by using biosolid.* Global Nest J, 2006. **8**(2): p. 113-120.

106. Dod, R., G. Banerjee, and S. Saini, *Adsorption of methylene blue using green pea peels (Pisum sativum): a cost-effective option for dye-based wastewater treatment.* Biotechnol. Bioprocess Eng., 2012. **17**(Copyright (C) 2013 American Chemical Society (ACS). All Rights Reserved.): p. 862-874.

107. Yao, Y., et al., *Adsorption behavior of methylene blue on carbon nanotubes.* Bioresource Technology, 2010. **101**(9): p. 3040-3046.

108. Yasin, Y., M.Z. Hussein, and F.H. Ahmad, *Adsorption of methylene blue onto treated activated carbon.* The Malaysian journal of analytical sciences, 2007. **11**(11): p. 400-406.

109. Vadivelan, V. and K.V. Kumar, *Equilibrium, kinetics, mechanism, and process design for the sorption of methylene blue onto rice husk.* Journal of Colloid and Interface Science, 2005. **286**(1): p. 90-100.

110. Kavitha, D. and C. Namasivayam, *Experimental and kinetic studies on methylene blue adsorption by coir pith carbon.* Bioresource Technology, 2007. **98**(1): p. 14-21.

111. Salman, D.D., W.S. Ulaiwi, and N. Tariq, *Determination the Optimal Conditions of Methylene Blue Adsorption by the Chicken Egg Shell Membrane.* International Journal of Poultry Science, 2012. **11**(6): p. 391-396.

112. Tsai, W.-T., et al., *The adsorption of Methylene Blue from aqueous solution using waste aquacultural shell powders.* J. Environ. Eng. Manage, 2009. **19**(3): p. 165-172.

113. Diaz-Garcia, M.E., *Molecular Imprinting in Sol-Gel Materials: Recent Developments and Applications.* Mikrochimica acta (1966), 2005. **149**(1-2): p. 19-36.

114. Mudd, S., *A hypothetical mechanism of antibody formation.* The Journal of Immunology, 1932. **23**(6): p. 423-427.

115. Pauling, L., *Molecular architecture and biological reactions.* Chemical and engineering news, 1946. **24**(10): p. 1375-1377.

116. Pauling, L. and D.H. Campbell, *The manufacture of antibodies in vitro.* The Journal of experimental medicine, 1942. **76**(2): p. 211-220.

117. Sellergren, B., *Molecularly imprinted polymers: man-made mimics of antibodies and their application in analytical chemistry*. Vol. 23. 2000: Elsevier.

118. Komiyama, M., et al., *Molecular imprinting: from fundamentals to applications.* Molecular Imprinting: From Fundamentals to Applications, by Makoto Komiyama, Toshifumi Takeuchi, Takashi Mukawa, Hiroyuki Asanuma, pp. 148. ISBN 3-527-30569-6. Wiley-VCH, March 2003., 2003. **1**.

119. Komiyama, M., et al., *Fundamentals of molecular imprinting.* Molecular Imprinting: From Fundamentals to Applications, 2003: p. 9-19.

120. Slowing, I., *Mesoporous silica nanoparticles as controlled release drug delivery and gene transfection carriers ☆*. Advanced drug delivery reviews, 2008. **60**(11): p. 1278-1288.

121. Gong, C.B., *The Fabrication of a Photoresponsive Molecularly Imprinted Polymer for the Photoregulated Uptake and Release of Caffeine.* Advanced functional materials, 2006. **16**(13): p. 1759-1767.

122. Allender, C.J., et al., *Pharmaceutical applications for molecularly imprinted polymers.* International journal of pharmaceutics, 2000. **195**(1): p. 39-43.

123. Lee, S.C., H.M. Lin, and H. Chen, *Studies on the preparation and properties of inorganic molecularly imprinted polymer (MIP) based on tetraethoxysilane and silane coupling agents.* Journal of applied polymer science, 2009. **114**(6): p. 3994-3999.

124. Ye, L., R. Weiss, and K. Mosbach, *Synthesis and characterization of molecularly imprinted microspheres.* Macromolecules, 2000. **33**(22): p. 8239-8245.

125. Liu, X., et al., *Monolithic molecularly imprinted polymer for sulfamethoxazole and molecular recognition properties in aqueous mobile phase.* Analytica chimica acta, 2006. **571**(2): p. 235-241.

126. Lin, C.I., et al., *Synthesis of molecular imprinted organic–inorganic hybrid polymer binding caffeine.* Analytica chimica acta, 2003. **481**(2): p. 175-180.

127. Theodoridis, G. and P. Manesiotis, *Selective solid-phase extraction sorbent for caffeine made by molecular imprinting.* Journal of Chromatography A, 2002. **948**(1): p. 163-169.

128. Al-Oweini, R. and H. El-Rassy, *Surface characterization by nitrogen adsorption of silica aerogels synthesized from various $Si(OR)_4$ and $R''Si(OR')_3$ precursors.* Applied Surface Science, 2010. **257**(1): p. 276-281.

129. Al-Oweini, R., *Synthesis and characterization by FTIR spectroscopy of silica aerogels prepared using several $Si(OR)_4$ and $R''Si(OR')_3$ precursors.* Journal of molecular structure, 2009. **919**(1-3): p. 140-145.

130. Cenens, J. and R.A. Schoonheydt, *Visible spectroscopy of methylene blue on hectorite, laponite B, and Barasym in aqueous suspension.* Clays Clay Miner., 1988. **36**(Copyright (C) 2013 American Chemical Society (ACS). All Rights Reserved.): p. 214-24.

131. Ramadan, H., A. Ghanem, and H. El-Rassy, *Mercury removal from aqueous solutions using silica, polyacrylamide and hybrid silica–polyacrylamide aerogels.* Chemical Engineering Journal, 2010. **159**(1–3): p. 107-115.

132. Dong, D.C. and M.A. Winnik, *The Py scale of solvent polarities.* Canadian journal of chemistry, 1984. **62**(11): p. 2560-2565.

133. Langmuir, I., *The adsorption of gases on plane surfaces of glass, mica and platinum.* Journal of the American Chemical Society, 1918. **40**(9): p. 1361-1403.

134. Freundlich, H., *Of the adsorption of gases. Section II. Kinetics and energetics of gas adsorption. Introductory paper to section II.* Transactions of the Faraday Society, 1932. **28**: p. 195-201.

135. Temkin, M.I. and V. Pyzhev, *Kinetics of ammonia synthesis on promoted iron catalysts.* Acta Physicochim. URSS, 1940. **12**(Copyright (C) 2013 American Chemical Society (ACS). All Rights Reserved.): p. 327-56.

136. Dubinin, M.M. and L.V. Radushkevich, *The equation of the characteristic curve of activated charcoal.* Dokl. Akad. Nauk SSSR, 1947. **55**(Copyright (C) 2013 American Chemical Society (ACS). All Rights Reserved.): p. 327-9.

137. Redlich, O. and D.L. Peterson, *A useful adsorption isotherm.* Journal of Physical Chemistry, 1959. **63**(6): p. 1024-1024.

138. Toth, J., *Gas adsorption on solid surfaces of inhomogeneous activity. IV.* Acta Chim. Acad. Sci. Hung., 1962. **33**(Copyright (C) 2013 American Chemical Society (ACS). All Rights Reserved.): p. 153-63.

139. Sips, R., *On the structure of a catalyst surface.* The Journal of Chemical Physics, 1948. **16**: p. 490.

140. Sips, R., *On the structure of a catalyst surface. II.* The Journal of Chemical Physics, 1950. **18**: p. 1024.

141. Ho, Y., J. Porter, and G. McKay, *Equilibrium isotherm studies for the sorption of divalent metal ions onto peat: copper, nickel and lead single component systems.* Water, Air, and Soil Pollution, 2002. **141**(1-4): p. 1-33.

142. Foo, K.Y. and B.H. Hameed, *Insights into the modeling of adsorption isotherm systems.* Chemical Engineering Journal, 2010. **156**(1): p. 2-10.

143. Ho, Y.-S. and G. McKay, *Pseudo-second order model for sorption processes.* Process Biochemistry, 1999. **34**(5): p. 451-465.

144. Nollet, H., et al., *Removal of PCBs from wastewater using fly ash.* Chemosphere, 2003. **53**(6): p. 655-665.

145. Vimonses, V., et al., *Kinetic study and equilibrium isotherm analysis of Congo Red adsorption by clay materials.* Chemical Engineering Journal, 2009. **148**(2): p. 354-364.

146. Masterton, W.L., C.N. Hurley, and E.J. Neth, *Chemistry: principles and reactions*. 2011: CengageBrain. com.

147. Wei, H.-S., et al., *Preparation of inorganic molecularly imprinted polymers with higher adsorption and selectivity by sol–gel method.* Journal of Chromatography B, 2006. **836**(1): p. 57-62.